Image registration for dose accumulation between external beam radiotherapy and brachytherapy for cervical cancer: Comparison to clinical practice

Medet Zhanuzakov

Medical Physics Unit

McGill University

Montreal, Quebec, Canada

December 8, 2022

A thesis presented for the degree of Masters in Medical Radiation Physics

Table of contents

Abstract

Background: Locally advanced cervical cancer is currently treated with external beam radiotherapy (EBRT), brachytherapy (BT), and concomitant chemotherapy. According to GEC-ESTRO recommendations, a direct dose addition (DA) of the EBRT prescription dose and the BT dose volume histogram parameters (DVH) is adequate to record and report doses in the organs at risk (OAR) for small volumes. However, DA overestimates cumulative dose when hotspots do not overlap between fractions. To resolve these challenges, we studied the possibility to use deformable image registration (DIR) for dose summation. Furthermore, a way of comparing the BT treatment intensity is using isodose surface volumes (ISVs). ISVs have been a concept used since 2000, however, not widely used in the BT community. Based on the ICRU Report 89, advancements are now being made to gain an understanding of how to compute ISVs and their correlation with treatment morbidity. For this reason, the project will also include an analysis of several methods to compute ISVs.

Aim: To develop a methodology for DIR between EBRT and BT images, perform dose summation based on the deformation vector field and compare different isodose surface volume (ISVs) calculation approaches.

Materials and methods: Twenty patients with locally advanced cervical cancer (LACC) were studied in this thesis. Five of the twenty patients were randomly selected to perform the dose summation using DIR. Patients were treated with EBRT to a dose of 45 Gy in 25 fractions and 4 high dose rate (HDR) BT fractions. DIR was performed by using Velocity software v4.1 (Varian Medical Systems, Palo Alto, California, USA). All five patients had CT scans from the EBRT treatment and 2 MR image sets from the first (BT1) and third (BT3) BT fractions, corresponding to 2 different BT implants. Each BT implant was delivered over 2 fractions on consecutive days. DIR was performed between BT3 and EBRT images using deformable multi-

pass registration which is a three-pass image registration. DIR between BT3 and BT1 for both targets and organs-at-risk (OARs) was structure-based guided. DIR for bladder and rectum was structure-based using a burn-in feature that allowed overwriting the density value. The total equivalent dose based on DIR was obtained and compared with the DA method. HR-CTV and IR-CTV D100%, D98%, D90%, and D50% were compared. Bladder and rectum doses $D_{2\ cm^3}$ and $D_{0.1\ cm^3}$ were compared. The ISVs encompassed by 85 Gy, 75 Gy, and 60 Gy $EQD2_{10}$ were calculated with three different approaches. The first approach was to extract the ISVs of the given EQD2 dose level from the treatment planning system (ISV_{TPS}) on BT1 and BT3 MR images. The second approach was to use a predictive model (ISV_{Pred}) based on BT's Total Reference Air Kerma (TRAK). The third approach computed ISVs based on the rigid image registration between BT3 and BT1/EBRT images (ISV_{Reg}). Qualitative validation of DIR was performed by using dice similarity coefficient (DSC) and mean distance to agreement (MDA).

Results: The DIR provided a mean DSC of 0.9 for bladder, 0.9 for rectum, 0.8 for HR-CTV, and 0.9 for IR-CTV. Average MDA value was 0.7 mm for bladder, 1.1 mm for rectum, 1.4 mm for HR-CTV, and 1.7 mm for IR-CTV. According to the TG-132 recommendations, DSC should be 0.8, and MDA should be 2-3 mm. HR-CTV doses calculated by the DIR method were higher by 1.2% for D100%, 1.8% for D98%, 1.5% for D90%, and 1.6% for D50% as compared to the DA method. A similar trend was seen when IR-CTV doses were evaluated. The cumulative IR-CTV D100% was 2.2% and, IR-CTV D98% was 1.93% greater compared to the DA approach. The accumulated dose calculated by DIR for the bladder $D_{2\ cm^3}$ and bladder $D_{0.1\ cm^3}$ was 7% and 6.7% lower, respectively, compared to the DA method. ISV calculation by the three different methods showed that the difference between approaches was not clinically significant. The average percent difference between the ISV_{TPS} and ISV_{Pred} was – 4.40% for 85 Gy, -3.29% for 75 Gy, and -3.04% for 60 Gy. The average difference between ISV_{TPS} and ISV_{Reg} was – 4.68% for 85 Gy, -4.77% for 75 Gy, and -4.21% for 60 Gy. The

average difference between ISV_{Reg} and ISV_{Pred} was 0.28% for 85 Gy, 1.48% for 75 Gy, 1.16% for 60 Gy.

Conclusion: Although DIR validation by use of DSC and MDA met the TG-132 recommendations, we do not recommend using the DIR method in the clinic. ISV_{TPS}, ISV_{Pred}, and ISV_{Reg} could be equally used to assess the isodose surface volume.

Abrégé

Le cancer du col de l'utérus localement avancé est actuellement traité par radiothérapie externe (EBRT), curiethérapie (BT) et chimiothérapie concomitante. Selon les recommandations du GEC-ESTRO, une simple addition directe (AD) de la dose de prescription d'EBRT et des paramètres d'histogramme dose-volume (DVH) de BT est considéré adéquat pour enregistrer et rapporter les doses dans des petits volumes des organes à risque (OAR). Cependant, AD surestime la dose cumulée lorsque les regions à dose élevées (hot-spots) ne se superposent pas entre les fractions. Pour résoudre ces problèmes, nous avons étudié la possibilité d'utiliser le enregistrement d'image déformable (EIR) pour l'addition de dose. Un moyen de comparer l'intensité du traitement BT consiste à utiliser des volumes de surface isodoses (VSI). Les VSI sont un concept utilisé depuis 2000, mais pas largement utilisé dans la communauté BT. Basé sur le rapport ICRU 89, on peut maintenant mieux comprendre comment calculer les VSIs et leur corrélation avec la morbidité liée au traitement. Pour cette raison, le projet comprendra également une analyse de plusieurs méthodes de calcul des VSI.

Objectifs: Développer une méthodologie pour un EIR entre les images EBRT et BT, effectuer une AD basée sur le champ de vecteurs de déformation et comparer plusieurs méthodes de calcul des VSI.

Matériels et méthodes: Vingt patientes atteintes d'un cancer du col de l'utérus localement avancé (LACC) ont été étudiées dans cette thèse. Cinq des vingt patients ont été sélectionnés au hasard pour effectuer la addition des doses à l'aide de EIR. Les patients ont été traités par EBRT à une dose de 45 Gy en 25 fractions et 4 fractions BT à haut débit de dose (HDR). L'EIR a été réalisée à l'aide du logiciel Velocity v4.1 (Varian Medical Systems, Palo Alto, Californie, États-Unis). Les cinq patients ont eu des simulations CT virtuels du traitement EBRT et deux ensembles d'images IRM pour la première (BT1) et troisième (BT3) fractions BT,

correspondant à deux implants BT différents. Chaque implant BT a été délivré en 2 fractions sur des jours consécutifs. L'EIR a été réalisé entre les images BT3 et EBRT à l'aide d'un enregistrement multipasse déformable qui est un enregistrement d'image en trois étappes. L'EIR entre BT3 et BT1 pour les cibles et les OAR était guidé par les contours des organes. L'EIR pour la vessie et le rectum étaient basés sur les contours des organs à l'aide d'une fonction de rodage qui permettait changer la valeur de densité. La dose équivalente totale basée sur l'EIR a été obtenue et comparée avec la méthode AD. HR-CTV et IR-CTV D100 %, D98 %, D90 % et D50 % ont été comparés. Les doses de la vésie et rectum $D_{2\ cm^3}$ et $D_{0.1\ cm^3}$ ont été comparées. Les VSI définiés par les doses de 85 Gy, 75 Gy et 60 Gy $EQD2_{10}$ ont été calculés avec trois approches différentes. La première approche consistait à extraire les ISV d'un niveau de dose EQD2 donné du système de planification de traitement (VSI_{TPS}) sur les images MR BT1 et BT3. La deuxième approche consistait à utiliser un modèle prédictif (VSI_{Pred}) basé sur le Total Reference Air Kerma (TRAK) de BT. La troisième approche a calculé les VSI sur la base du recalage d'image rigide entre les images BT3 et BT1/EBRT (VSI_{Reg}). La validation qualitative du EIR a été effectuée en utilisant les "Dice Similarity Coefficient" (DSC) et la "Mean Distance to Agreement" (MDA).

Résultats: Des DSC moyens de 0,9 pour la vessie, 0,9 pour le rectum, 0,8 pour HR-CTV et 0,9 pour IR-CTV ont été obtenus après l'utilisation de l'EIR. La valeur moyenne de MDA était de 0,7 mm pour la vessie, 1,1 mm pour le rectum, 1,4 mm pour HR-CTV et 1,7 mm pour IR-CTV. Selon les recommandations du TG-132, le DSC doit être de 0,8 et le MDA de 2 à 3 mm. Les doses HR-CTV calculées par la méthode EIR étaient plus élevées de 1,2 % pour la quantité D100 %, 1,8 % pour D98 %, 1,5 % pour D90 % et 1,6 % pour D50 % par rapport à la méthode AD. Une tendance similaire a été observée lorsque les doses IR-CTV ont été évaluées. Le IR-CTV D100 % était de 2,2 % et IR-CTV D98 % était supérieur de 1,93 % par rapport la méthode AD. La dose cumulée calculée par EIR pour la vessie $D_{2\ cm^3}$ et la vessie $D_{0.1\ cm^3}$ était

inférieure de 7 % et 6,7 %, respectivement, à la méthode AD. Le calcul de l' VSI par les trois méthodes différentes a montré que la différence entre les méthodes n'était pas cliniquement significative. La différence moyenne en pourcentage entre l'VSI_{TPS} et l'VSI_{Pred} était de – 4,40 % pour 85 Gy, -3,29 % pour 75 Gy et -3,04 % pour 60 Gy. La différence moyenne entre VSI_{TPS} et VSI_{Reg} était de – 4,68 % pour 85 Gy, -4,77 % pour 75 Gy et -4,21 % pour 60 Gy. La différence moyenne entre VSI_{Reg} et VSI_{Pred} était de 0,28 % pour 85 Gy, 1,48 % pour 75 Gy, 1,16 % pour 60 Gy.

Conclusion: Bien que la validation EIR par l'utilisation de DSC et de MDA a satisfait les recommandations TG-132, nous ne recommandons pas l'utilisation de la méthode EIR dans la clinique. VSI_{TPS}, VSI_{Pred} et VSI_{Reg} pourraient également être utilisés pour évaluer le volume de surface isodose.

Acknowledgements

I would like to appreciate and give my warmest thank you to my supervisor, Monica Serban. The completion of my study could not have been possible without her supervision and guidance. I am grateful for her patience and support. It was a pleasure to work under her supervision.

Also, I would like to thank Jan Seuntjens for his financial support through my studies. Separate gratitude towards Georges Al Makdessi for providing us access to the Velocity software.

Special thanks to my beautiful and lovely wife, Assem. I am thankful for supporting, taking care, and believing in me, even when I lost belief in myself. I love you.

Big thanks to my brothers, little sister, Mom and Dad for their continuous support and belief in me.

List of Figures

List of Tables

List of Acronyms

BT	Brachytherapy.
CTV	Clinical Target Volume.
DA	Direct Dose Addition.
DIR	Deformable Image Registration.
DSC	Dice Similarity Coefficient.
DVH	Dose Volume Histogram.
EBRT	External Beam Radiotherapy.
HDR	High Dose Rate.
HR-CTV	High Risk Clinical Target Volume.
HWT	Height, Width, And Thickness.
IR-CTV	Intermediate Risk Clinical Target Volume.
ISV	Isodose Surface Volume.
LACC	Locally Advanced Cervical Cancer.
LQ	Linear Quadratic.
MDA	Mean Distance to Agreement.
OAR	Organs-At-Risk.
OHD	Overlapping High Dose Volumes.
PTV	Planning Target Volume.
TRAK	Total Reference Air Kerma.
TRE	Target Registration Error.
UD	Uniform Dose.

Chapter 1

1.1 Introduction

1.1.1 Background

Cervical cancer is the fourth most common cancer and the fourth greatest cause of cancer death in women, with an expected 604,000 new cases and 342,000 deaths worldwide in 2020. It is one of the few cancers caused by a virus and therefore preventable. While increased vaccination and screening programs are implemented and popularized in developing countries, causing the number of cases to decrease, cervical cancer remains a significant problem in less developed parts of the world. It is therefore important to continue to develop the treatment recommendations to avoid significant side effects.

Figure 1 shows the incidence and mortality for cervical cancer by region [1]. Age-standardized rate per 100 000 is weighted by averaging the number of mortality rates per age group per 100 000 persons. According to figure 1, the eastern Africa region has the highest incidence and mortality rates, with 40.1 and 28.6, respectively. On the other hand, the western Asia region has the lowest incidence and mortality, 4.1 and 2.3, respectively. Meanwhile, most European regions have 7-10 incidences per 100 000 people, and the mortality rate is approximately 2 per 100 000 people.

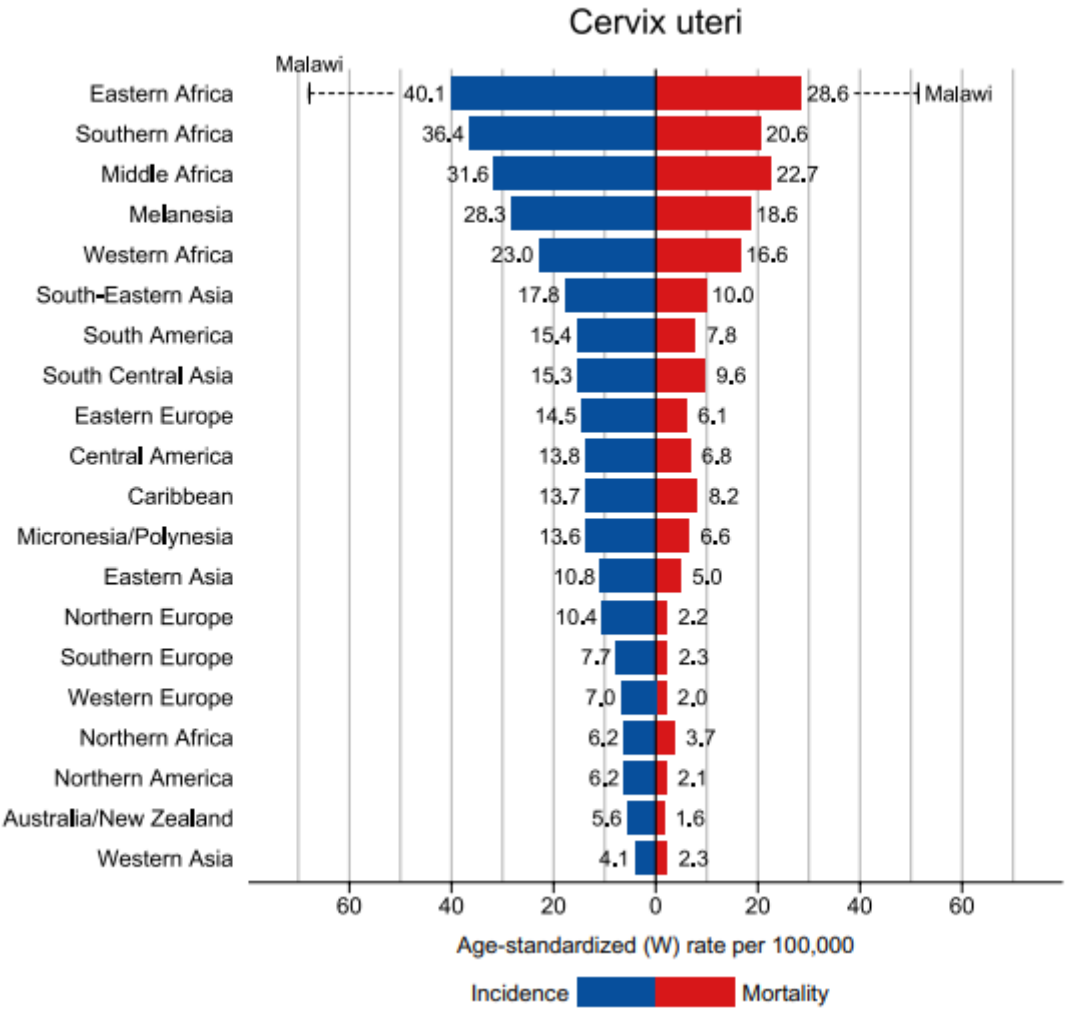

Figure 1. Age-Standardized Rates of Incidence and Mortality for Cervical Cancer by Region in 2020. Source: GLOBOCAN 2020 [1].

1.1.2 Locally advanced cervical cancer treatment

Locally advanced cervical cancer (LACC) is currently treated with a combination of external beam radiotherapy (EBRT) and concomitant chemoradiotherapy followed by a boost to the residual tumor using brachytherapy (BT). EBRT is the first part of the treatment, with the goal of delivering the prescribed dose to the primary tumour and elective nodes [3]. ICRU Report 50 defines the planning target volume (PTV) as a geometrical concept used to determine optimal beam configurations, considering the net effect of all potential geometrical variations, such that the prescribed dose is absorbed in the clinical target volume (CTV) [4]. In EBRT, the

radiation source is placed at a specified distance outside of the patient, and typically delivered by a linear accelerator. In this type of treatment, the photon beams travel from the source through the body to deposit energy in the target volume. Chemotherapy is the use of medications to destroy cancer cells, with systemic consequences [5]. BT is the second part of treatment, with the aim of locally treating the residual tumor remaining after EBRT [3]. BT refers to the treatment of cancer using radiation from small, encapsulated radionuclide sources at close range. The dose is then delivered constantly, either for a short amount of time (temporary implants) or for the duration of the source's lifespan until total decay (permanent implants). The source of radiation is introduced by a computer-controlled machine (an afterloader) into hollow channels (needles, tubes, guides), placed manually by a radiation oncologist inside the tumour tissue (interstitially – IS) or in a body cavity next to the tumour (intracavitary – IC). The channels are collectively called “applicators” and their configuration inside the patient is called “implant”. In this type of radiotherapy, irradiation is delivered from inside the body over a short distance and deposited in the tissue close to the applicators thereby forming a steep dose gradient. Fractionating radiation treatment is delivering radiation across several weeks rather than in a single session and administered to improve the therapeutic ratio [5]. Fractionated radiation is based on five biological factors of radiotherapy [5]:

1. Radiosensitivity – different organs and tissues have different sensitivity to radiation.
2. Repair – irradiated cells can repair fractionated radiation damage.
3. Repopulation – between a fractionated radiation therapy session, cells can repopulate.
4. Redistribution – the cell death from a fractionated therapy is increased by redistribution in populations of proliferating cells throughout the cell cycle stages.
5. Reoxygenation – reoxygenation process of hypoxic cells increases their sensitivity to the radiation.

In LACC, both forms of irradiation are combined, typically in a sequence of 25 daily fractions of EBRT over 5 weeks, followed by a sequence of 2 to 5 fractions of BT. BT has been a fundamental component in the effective treatment of LACC for more than 100 years, and was the first form of radiotherapy ever practiced. BT accounts for about half of the total dose delivered to the periphery of the residual tumour.

1.1.3. Modern brachytherapy: dose recording and reporting

In the late 1990s, the BT treatment evolved considerably in terms of imaging modalities and magnetic resonance imaging – guided adaptive brachytherapy (MRI-GABT) was pioneered in cervix cancer. MRI, with its excellent soft tissue-contrast, constituted a superior modality for tumour assessment. Recommendations by the GEC-ESTRO [2] introduced the concepts of MRI-based adaptive and risk-related target volumes in LACC according to the number of clonogenic tumor cells expected to survive after initial EBRT and concomitant chemotherapy: gross tumour volume (GTV_{res}), high risk and intermediate risk clinical target volume (CTV_{HR} and CTV_{IR}). The GTV_{res} corresponds to the residual high signal regions on T2w MRI at time of BT, the CTV_{HR} includes the GTV_{res} plus residual pathological tissue in the areas where initial GTV has regressed (grey zones on MRI) plus the entire uninvolved cervix. CTV_{IR} is in principle CTV_{HR} plus a margin and corresponds to the region of the macroscopic disease at diagnosis (the initial primary tumour).

A common approach for cumulative dose reporting from EBRT and BT was initiated based on the linear-quadratic (LQ) model with calculation of a biologically equivalent dose in 2 Gy fractions (EQD2) using $\alpha/\beta = 10$ Gy for tumour effects, $\alpha/\beta = 3$ Gy for late normal tissue damage for pulsed dose rate (PDR) BT (Equation1) [6].

$$EQD2 = D\left(\frac{d + \frac{\alpha}{\beta}}{2 + \frac{\alpha}{\beta}}\right) \quad (1)$$

where D – total dose, d – dose per fraction, α – linear component of cell killing, β – quadratic component of cell killing, $\frac{\alpha}{\beta}$ – the dose at which both components are equal.

Point doses (e.g., bladder/rectum ICRU points) or reference volumes (e.g., V60Gy) that had been used for plan evaluation were supplemented by dose-volume reporting metrics such as D90%, D100% for target volumes and $D_{2\ cm^3}$, $D_{0.1\ cm^3}$ for OARs [7]. Prescribing, recording and reporting in cervix cancer BT was further developed and recently published by the ICRU and GEC-ESTRO as ICRU/GEC-ESTRO Report 89 [7].

The dose summation from EBRT and each BT fraction is typically performed by DA of the prescribed EBRT dose with different BT dose parameters such as $D_{2\ cm^3}$ or $D_{0.1\ cm^3}$ expressed in EQD2. DA method is the summation of cumulative biologically weighted dose from BT fractions with the biologically weighted dose from EBRT to calculate the total biologically weighted dose. The method of DA represents the worst-case scenario because it assumes that the high-dose region from the first fraction is at the same location as consecutive fractions, i.e., will lead to overlapping high-dose regions. However, high-dose region from BT fractions may not be at the same location during the treatment period, because of the tumor shrinkage, applicator insertion or bladder and rectum fillings. Nevertheless, this method was found to be accurate for bladder and rectum [7] but overestimates the doses to the sigmoid and bowel because the position of these organs is moving and changes from fraction to fraction [7]. Larger OAR volumes irradiated to intermediate dose levels have been shown to be predictors of morbidity, although the evidence is somewhat limited [7]. Ideally, cumulative EBRT+BT doses to larger organ volumes (than 2 cm^3) should be evaluated as well. However, DA method, in this case, would result in high uncertainties and unreliable results due to different OAR volumes and positions from fraction to fraction as well as due to the BT

applicator which is not present during the EBRT treatment. Therefore, doses to larger organ volumes are currently assessed for the EBRT plan only.

1.2 Motivation of the project

According to GEC-ESTRO recommendations [2], a DA of the EBRT prescription dose and the BT dose-volume histogram (DVH) parameters is adequate to record and report hot-spot doses in the organs at risk (OAR) and calculate the total equivalent dose in 2 Gy per fraction from EBRT and BT. However, the DA method overestimates cumulative dose when hotspots from fraction to fraction are not in overlapping locations. We studied the potential of DIR to resolve these challenges. Because of the deformable nature of soft tissue, rigid registration between EBRT and BT images often results in low image registration accuracy and is unreliable [8]. My thesis aims to develop a methodology for DIR between EBRT and BT images and perform dose summation based on deformed images. This is done to enable a comparison of different isodose surface volume (ISVs) calculation approaches. The ISVs encompassed by 85 Gy, 75 Gy, and 60 Gy $EQD2_{10}$ were calculated with three different approaches. The first approach was to read the ISVs of the given EQD2 dose level in the treatment planning system (ISV_{TPS}) on BT1 and BT3 MR images. The second approach was to use a predictive model (ISV_{Pred}) based on BT's Total Reference Air Kerma (TRAK). The third approach computed ISVs based on the rigid image registration between BT3 and BT1/EBRT images (ISV_{Reg}).

Chapter 2 overviews DIR, the physical aspects of image registration, and the process of validation of image registration, and provides information about Velocity software v4.1 (Varian Medical Systems, Palo Alto, California, USA), clinical aspects of dose reporting, challenges of DIR and relevant literature review. Chapter 3 summarizes DIR approaches and accuracy, ISVs calculation, and doses to targets and OAR. Chapter 4 reports the results of DIR approach accuracy, doses to HR-CTV, IR-CTV, bladder, and rectum from the DIR for cervical

cancer, and ISVs for 85 Gy, 75 Gy, and 60 Gy EQD210. Chapter 5 provides a discussion of the results, and chapter 6 concludes the thesis.

Chapter 2

2.1 Deformable image registration

Image registration is the process of matching an image to a reference (or target) image and determining the mathematical transformation to achieve this goal. The number of degrees of freedom, in coordinate transformation, is determined by the type of image registration. With degrees of freedom in the coordinate transformation we mean, for example, rotation (yaw), tilt and roll represent 3 degrees of freedom, whereas translation represents another three degrees of freedom. There are three types of image registration. Rigid registration consists of 6 degrees of freedom with three rotations and three translation parameters. In rigid image registration, all pixels move uniformly such that each pixel-to-pixel relationship stays consistent during the transformation. Affine registration consists of 9-12 degrees of freedom in addition to the rotation and translation parameters also allow uniform scaling and sheering. Deformable registration has a degree of freedom which is three times the number of voxels in an image and allows shrinkage and stretching. In DIR, the pixel-to-pixel relationship changes. DIR results in a deformation vector field that specifies the correspondence between the reference and moving images [9, 10].

2.1.1 Physics aspects of image registration

Image registration is the process of determining the optimal alignment between the homologous points in one image set to points in another image set. There are three main components in any image registration algorithm.

1) Geometric transformation T which is a function that applies to the moving image to align it to the stationary image. The primary goal of image registration is to determine the transformation T.

$$X_B = T(X_A, \{\beta\}) \quad (2)$$

where,

X_A – the position of a point within the moving image,

X_B – is the coordinate of the same point in the stationary image,

$\{\beta\}$ – the set of parameters defining the transformation.

2) A registration metric that assesses the degree of alignment between two images. Registration algorithms may be categorized into two major groups depending on their nature: geometry-based metrics and intensity-based metrics. Geometric metrics use anatomical or organ boundaries and artificial landmarks, while intensity metrics use image voxel intensity data. Point-to-point or surface-to-surface matching are the most prevalent geometry-based registration metrics. The registration metric for point matching is defined by the coordinates of pairs of identical points in the image versus reference image. These points might represent anatomic landmarks or fiducial markers. The registration metric R is equal to the sum of the squared distances between matching points, where N is the number of points.

$$R = \sum \frac{(p_{A'} - p_B)^2}{N} \quad (3)$$

where,

$p_{A'}$ – the coordinates of pairs of corresponding points from transformed image

p_B – the coordinates of pairs of corresponding points from reference image

Surface matching does not need a one-to-one correlation of precise points; instead, it seeks to maximize the overlap between related points.

Intensity-based DIR is used to get around some of the limitations of utilizing explicit geometric features to register image data. Similarity metrics compare the distributions of matching voxel values from the reference image with a transformed version of image to be registered. This similarity is measured using a variety of mathematical formulations. The sum of squared differences, cross-correlation and mutual information are the most often used similarity metrics in clinical practice. The sum of squared differences (SSD) metrics is computed as the average squared intensity (I_A and I_B) difference between the image to be registered and the reference image, where N is the number of voxels evaluated

$$SSD = \frac{\sum(I_{A'} - I_B)^2}{N} \quad (4)$$

where,

$I_{A'}$ – intensity of transformed image.

I_B – intensity of reference image

This metric is straightforward to calculate and successfully registers two imaging studies on single modality images (e.g., CT to CT) with identical intensities for the corresponding anatomy.

An alternate method employs the cross-correlation (CC) metric, which quantifies the similarity of the image signals in two images. Cross-correlation registration optimizes the intensity product as opposed to reducing intensity difference. This metric's limitation is its sensitivity to changes in the voxel value. This metric is effective for single-modality images and potentially a tiny region of multimodality images.

Registration metrics based on simple differences or products of intensities are ineffective for data from different modalities where the pixel intensities of the relevant anatomy are often different. In such situations, complex metrics based on intensity statistics are preferable. Using these metrics has no dependency on the absolute intensity values. Mutual information (MI) is one such metric that has proved quite successful for registering image data from various

modalities. Mutual information attempts to align voxels whose values have identical probabilities of occurrence in their respective image sets.

$$MI(I_{A'}, I_B) = \sum_B \sum_A P(I_{A'}, I_B) \log_2 [p(I_{A'}, I_B)/p(I_{A'})p(I_B)] \quad (5)$$

where,

$I_{A'}$ – intensity of transformed moving image.

I_B – intensity of stationary image

Mutual information is the best intensity-based similarity metric for images of different modalities.

3) The optimizer. The optimizer aims to identify the optimal set of parameters for the transformation that yields the optimal image alignment as evaluated by the similarity metric. For image-based similarity metrics, most optimizers are iterative and will repeatedly test various transformation parameters until the final value of the similarity metric converges to an optimal value. Several methods, including gradient and stochastic-based approaches, are used. It is essential to comprehend the optimization approach to understand its convergence and potential dangers [10].

2.1.2 Validation of deformable image registration

Each voxel irradiated by EBRT should be matched with its corresponding voxel irradiated by BT while conducting deformable dose accumulation of EBRT and BT. This assumption is often broken due to differences in intestinal gas, bladder filling, tumor shrinkage or tumor growth, etc. and the presence of BT applicator and vaginal packing, which may result in high uncertainty and implausible solutions for DIR. The challenges of DIR will be discussed later. It is essential to define the terminology used to explain image registration quality assurance.

A) Validation refers to examining the process and toolset to confirm that valid image registration can be consistently done for the intended application.

B) Verification is the process of validating that the accuracy of a specific image registration is sufficient for the intended use.

C) Quality Assurance refers to the methods and processes put in place to ensure that each image registration is performed following systematic, well-documented and vetted protocols [10] and that changes in performance metrics are compared to accepted tolerances and action levels.

2.1.3 Quality assurance of deformable image registration

Image registration accuracy might be validated either with quantitative or qualitative measures. Quantitative validation is required for the initial commissioning of an image registration software. Qualitative verification of image registration is necessary to guarantee that the registration is clinically acceptable [10].

2.1.4 Quantitative verification

The alignment of anatomy or structures delineated in stationary image overlaid over the transformed image may give a qualitative assessment of registration accuracy. Under ideal conditions of registration and delineation, the anatomical contour of stationary image should correspond to that of the transformed image. In reality, there will not be an exact match due to contour variation. Variation in contour is dependent on the imaging modality and the structure of interest. Examples of quantitative image registration metrics are DSC, mean distance to agreement (MDA), target registration error (TRE) and the Jacobian determinant.

A) The dice similarity coefficient (DSC) is defined as the ratio of twice the volume of the intersection of two contours and the total volume of the union of two contours. As the contours approach agreement, the DSC value approaches 1; as the volumes split into two structures that do not overlap, the DSC value approaches 0.

$$DSC = \frac{2A \cap B}{A \cap B} \quad (6)$$

where,

A – target region of moving image

B – target region of stationary image

$\cap$ - intersection of two regions

B) Mean distance to agreement (MDA) evaluates the alignment of structures. To calculate the MDA, the contour of the stationary image would be converted into a sequence of points, and the distance between each point and the contour of the image to be registered is determined. After the contour of the transformed image is converted into points, the distance between each point and the reference contour image is determined. The mean distance to the agreement is then determined by averaging all distances.

C) Target registration error (TRE) is the average residual error between the identified points in a reference image and the identified points in the image, a transformed moving image created with the image registration. A 'perfect' registration at the landmark location would result in the identical spatial location of the landmark in both transformed image and reference image, yielding a TRE of 0. It may be challenging to describe the appropriate matching points precisely and adequately, especially when recording multimodality data.

$$TRE = \sqrt{(\Delta x)^2 + (\Delta y)^2 + (\Delta z)^2} \quad (7)$$

where,

Δx – the difference between x coordinates of each homologous point pairs.

Δy – the difference between y coordinates of each homologous point pairs.

Δz – the difference between z coordinates of each homologous point pairs.

D) The Jacobian determinant indicates the local volume change of voxels resulting from the registration. Greater-than-1 Jacobian determinants imply volume expansion, between 0 and 1

suggest volume contraction, a value of 1 indicates no change, and a value of less than or equal to 0 implies nonphysical deformation. A Jacobian determinant of less than or equal to zero suggests an incorrect physical model of the patient. It may indicate a registration mistake or a restriction in the algorithm's handling of complicated deformation [10].

2.1.5 Qualitative verification

There are several standard techniques to perform qualitative validation (Figure 2).

A) Split-screen, floating window, and checkerboard displays are used for identifying registration issues in clinical settings. They are especially good at detecting mismatches between related structures at high contrast tissue surfaces.

B) Image overlay displays images that are a blended composition of registered images. The reference image is often shown in a grayscale colour map, while the floating image is displayed on a colour scale.

C) Difference image displays help visualize intramodality registration accuracy. Subtraction of registered voxel intensities produces the display. If the absolute value of the difference is utilized, a perfect intensity match at the voxel level results in a display level of 0 (black); as the mismatch increases, the projected colour for the voxel approaches white.

D) Contour overlays are helpful for multimodality image registration. Anatomical outlines produced on one imaging modality may then be overlaid on the second imaging modality in the exact spatial location [10].

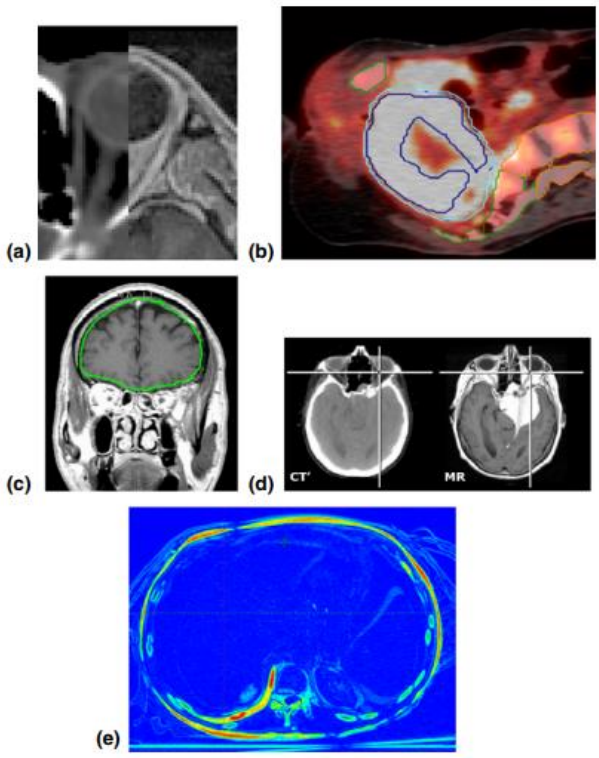

Figure 2. A) (a) Visual image validation using split screen displays. (b) Image overlay displays (c) Contour mapping displays. (d) Side-by-side display with the linked cursor. (e) Difference images are displays. Source: TG-132 [10].

2.2 Velocity™ software

Velocity's image registration aims to align patient anatomy by simulating displacement and volume change. This is achieved by deforming the voxels of one image set to fit another primary image's anatomy, producing a deformation matrix. Nonetheless, the clinical stability of the DIR is affected by several variables, including the algorithm's degrees of freedom, input image quality, and method of regularization. The DIR algorithms follow the same basic principles stated in chapter 2.1.1. A regularization function provides a smooth deformation vector field to mimic tissue structure and physiological movement or deformation. Constrained regularization prevents a voxel from moving independently from its neighbor pixels and requires congruent movement between neighboring voxels. In contrast, unconstrained

regularization permits voxels to move independently, possibly jumping over one another, causing tears and folds in the deformation grid (Figure 3).

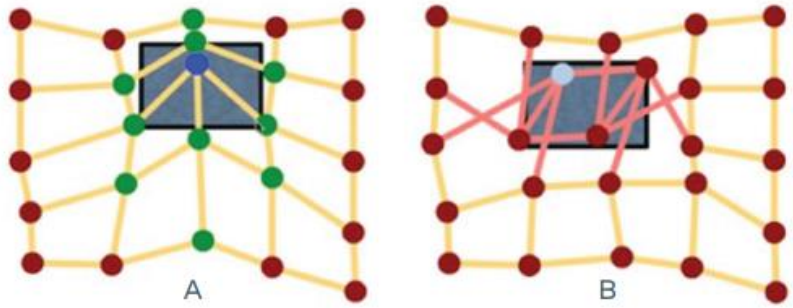

Figure 3. Constrained regularization (A) compared to unconstrained regularization (B) Source: Fox et al. [11].

The Velocity software employs an elastic B-spline algorithm, and mutual information as the cost function metric. B-spline registration is a deformable registration method that utilizes B-spline curves to build a continuous deformation field that maps each voxel in a image to be registered to a matching voxel in the reference image [12]. The mutual information metric, discussed in chapter 2.1.1, of Velocity calculates the marginal and joint probability density functions of the volumes over a subset of voxels, enabling the optimizer to determine the correct convergence. Marginal and joint probability density functions are used to align voxels that have the same intensity and high probability to be at the same region at the same time irrespective of other variables. This mutual information metric adjusts inherently for noise, artifacts, and other factors that decrease image quality. Additionally, it allows Velocity to register multimodal image volumes. The degrees of freedom may be modified, allowing for a change from a rigid to a highly elastic motion through single-pass, multi-pass, or extended multi-pass deformation. A deformable single-pass image registration runs image registration only once. A deformable multi-pass is a three-pass image registration with better resolution than a single pass. An extended multi-pass is a six-pass deformable that uses finer resolution than a deformable multi-pass. Velocity also includes a structure-guided deformable, a hybrid method that combines the elastic B-spline with delineated contours of organs for large

deformation, such as bladder filling. Prudent judgment is required when trying to match the small details of two images when image similarity or acquisition quality is poor. The elastic technique used by Velocity seeks to reduce the number of errors exceeding a predefined threshold, while producing a satisfactory fusion with a smooth deformation field [11].

2.3 Clinical practice of dose recording and reporting

2.3.1 CTV_{HR} and CTV_{IR}

The ICRU-89 report recommends target doses reported to D98%, D90%, and D50%, which represent minimum doses delivered to the most irradiated 98%, 90%, and 50% of the target volume. Due to the interobserver variations for target delineation and due to the strong BT dose gradient, D100% is not reliable. Moreover, the target minimum absorbed dose depends on volume reconstruction and absorbed-dose sampling in the treatment planning system. A more reliable statistic is the near-minimum dose of D98%, in which 2% of the target volume receives a dose below this threshold. D50% indicates the dose provided to 50% of the target volume [7]. D90% is less susceptible to target contouring and is thus seen as a more "stable" parameter. Moreover, CTV_{HR} D90% has been shown to correlate with tumor control [7]. Target D90% is highly recommended for reporting and the clinical evidence has been established. It can be easily calculated from a DVH and converted to biologically weighted EQD2 doses, making them suitable for correct plan comparison across all dose rates and fractionation schedules.

V100% represents the volume encompassed by the prescription dose. V100% is based on the specified physical dose and therefore cannot be used for intercomparison between patients treated with different schedules and prescription doses. V100% can only be used to compare plans for the same patient or in a series of patients treated with the same dose and fractionation. The intercomparison issue is eliminated when biologically equivalent doses are employed (e.g., V60 Gy EQD2, V85 Gy EQD2). However, since the latter utilizes the cumulative doses of all

fractions, this parameter is only used for assessment after the final fraction in fractionated treatment [7].

2.3.2 Bladder and Rectum

Due to the heterogeneity of dose absorbed within organ walls, providing at least two dose–volume values in the high-dose area are recommended. The dose values $D_{0.1cm^3}$ and D_{2cm^3} reflect the lowest doses to the most irradiated 0.1 cm^3 and 2 cm^3 volumes of OAR, respectively. The GEC ESTRO GYN group recommended these OAR dose-volume parameters, $D_{2\ cm^3}$ and $D_{0.1\ cm^3}$ in 2006. $D_{2\ cm^3}$ has been shown to be predictive of morbidity in bladder, bowel, and rectum [7].

2.4 Isodose surface volume

The ISV refers to the volume encompassed by an isodose surface. The dose levels are selected to be clinically relevant for tumour control or for the development of normal tissue complications. ISVs can be used to compare among institutions or to track the transition from institutional standard loading to optimized treatment plans within a single institution. Certain absolute dose levels may be kept for reporting and following the planning procedure from the first treatment. The volume of an isodose surface should correspond to a dose judged representative of a specific clinical effect. ISVs based on the model are estimated by using Nkiwane et al. [13, 14] model.

$$ISV = 4965\left(\frac{TRAK}{d_{ref}}\right)^{\frac{3}{2}} + 170\left(\frac{TRAK}{d_{ref}}\right) - 1.5 \qquad (8)$$

where,

$TRAK$ – the fractional Total Reference Air Kerma of the BT

d_{ref} (Gy) – the fractional physical BT dose corresponding to the total EBRT and BT EQD2 dose level.

The TRAK is the integral of the reference air-kerma rate from all sources at 1 m from the source during the period of the treatment. TRAK is a purely physical parameter that cannot be directly correlated with a specific biological effect due to the fact that it does not account for the absorbed-dose distribution, fraction size, or absorbed-dose rate [7]. Air kerma is the amount of kinetic energy (in Joules) transferred from x-ray photons to electrons per kg of ionized air. Gray (Gy), which is equal to J/kg, is the SI unit for kerma [15].

2.5 Challenges of deformable image registration

We are confronted with challenges during the image registration and dose calculation processes. The most common challenge is the different treatment techniques of EBRT and BT. Both have different dose prescriptions and fractionations, which leads to different radiobiological effect and therefore the need to convert the fractional absorbed doses into EQD2. The next challenge is the presence of the applicator in the BT images, whereas the EBRT images do not have it. The presence of an applicator complicates image registration between BT and EBRT images, especially since rigid registration is not reliable. Rigaud et al. [3] analyzed organ volumes before BT and during BT. The vagina volume changed from 24.4 cm^3 without an applicator to 113.2 cm^3 with the applicator, representing a 528% expansion in volume of the vagina due to the presence of the applicator. Cervix and uterus decreased in volume by 4.8% and 2.2%, respectively. Bladder volume increased to 14.6%, while the rectum volume decreased to 6.4%.

2.6 Relevant literature review

Swamidas et al. [8] reviewed the current state of image registration for image-guided gynecological BT, in conjunction with EBRT. Based on the data from multiple studies, the

authors discussed the difference between deformable dose accumulation and DA for bladder and rectum for EBRT and BT. The dose derived from DA was subtracted from the one obtained from the DIR. The mean dose differences for bladder ranged between -3 Gy to 7 Gy, while for rectum, the difference ranged between -3 Gy and 9 Gy. The subtraction of DA from the deformable dose accumulation theoretically should be a negative value because direct addition represents a worst-case scenario. However, the difference was positive for some studies, illustrating the uncertainties in the deformable dose accumulation process due to errors in image registration. The authors reported that different DIR methods led to considerably different results that correlate poorly with the high dose regions predicted by contour- and intensity-based DIR [16]. The contour-based DIR method yielded consistent results, while the intensity-based method showed implausible results. It was also shown that the DA works well for bladder and rectum because the hotspots usually overlap partly or entirely. However, DA has limitations in determining the dose to the sigmoid and bowel since the locations of the hotspots are highly variable. They concluded that the present generation of DIR algorithms is insufficiently robust to manage the complexities of EBRT and BT dose accumulation.

Rigaud et al. [3] evaluated various image registration approaches for EBRT and BT. The authors analyzed rigid, intensity-based, structure-based, and hybrid image registrations. As an intensity-based DIR method, the Demons algorithm was applied. The ANACONDA algorithm was used as an intensity-based and hybrid DIR method. As a contour-based DIR, the MORFEUS algorithm was employed. Compared to rigid registration, the intensity-based DIR improved the DSC from 0.41 to 0.63 for bladder, from 0.41 to 0.57 for rectum, from 0.16 to 0.32 for cervix, from 0.21 to 0.43 for uterus, and from 0.26 to 0.42 for vagina. The structure-based DIR had a mean DSC of 0.96 for all organs. The authors showed that classical intensity-based and hybrid DIR methods could not sufficiently handle complex deformations. The biomechanical model-based approach was the only capable of matching organ contours, hence

deforming the dose more consistently and precisely. The difference between the dose calculated by MORFEUS and the planned dose at the time of BT for the bladder was 1.4 Gy for $D_{1\ cm^3}$ and 1.3 Gy for $D_{2\ cm^3}$, while for the rectum, it was 1.4 Gy for $D_{1\ cm^3}$ and 1.0 Gy for $D_{2\ cm^3}$. The authors concluded that intensity-based DIR was insufficient for estimating complicated deformations, but contour-based DIR may be used for this purpose.

Fox et al. [11] published a paper showing the evolution of Velocity and introduced a new Velocity software which uses an elastic B-spline algorithm and takes mutual information as a cost function. The mutual information metric calculates the volumes' marginal and joint probability density functions over a subset of voxels, enabling the optimizer to determine the correct convergence. The previous Velocity software used Fluid demons deformation, which allows voxels to move independently and unrestricted, and takes the similarity as the metric for the fusion optimization. Fluid demon deformation is very sensitive to noise and caused artifacts even for monomodal image registrations. To avoid this issue, the new Velocity software does not move voxels independently but instead moves in conjunction with neighboring voxels. The mutual information metric, because of its logarithmic terms, features a substantial noise compensation. The authors concluded that the Velocity B-spline algorithm's objective is to register the underlying anatomical structures while minimizing significant vector error magnitudes.

Heerden et al. [17] evaluated and compared different dose summation methods. They compared the DA methods, where we assume that EBRT has a uniform dose (UD) and DA with collecting the dose in the area of overlapping high dose volumes (OHD) with the DIR dose accumulation method. The DIR was performed using a Feature-Based DIR tool, provided by a research version of Oncentra Brachy. The mean DSC for bladder was 0.98 and for rectum 0.94. The mean dose to the bladder $D_{2\ cm^3}$ calculated by the DA approach was 69.8 Gy, while for UD and OHD approaches, it was 69.7 Gy and 71.6 Gy, respectively. The average dose to the rectum

$D_{2\,cm^3}$ was 59.6 Gy for the DA approach, 60 Gy for the UD approach, and 60.7 Gy for the OHD approach. The authors concluded that the UD method provided a better estimation than OHD, and the difference with DIR was insignificant. EBRT dose confirmed to be uniform.

Abe et al. [17] evaluated the usability of DIR in assessing the total cumulative dose of the BT and EBRT combinations. Image registrations were performed using MIM maestro. The rigid registrations based on bony anatomy were performed between fractions prior to DIR. The DIR dose accumulation results are compared with the direct addition method. The average DSC for the HR-CTV was 0.78, the rectum was 0.76, and the bladder was 0.87. The mean HR-CTV D90% and $D_{2\,cm^3}$ of the rectum and bladder were 81.4 Gy, 65.7 Gy, and 82.8 Gy with DIR and 83.1 Gy, 67.2 Gy, and 86.6 Gy with the DA method, respectively. The authors concluded that differences are insignificant, but there are some limitations in the accuracy of DIR.

Andersen et al. [18] demonstrated that the dose summation of DIR is dependent on the selection of the reference frame. If we use a bladder with a large volume as a reference frame and a bladder with a small volume as a moving image, the $D_{2\,cm^3}$ will be larger than if we use a bladder with a small volume as a reference. In this study, an MR image of BT3 was employed as a reference frame, and we did not choose a reference image based on the organ volumes.

In conclusion, all studies that compared the DIR approaches concluded that contour-based DIR provided more consistent results with higher accuracy. Swamidas et al. discussed that errors in image registration cause uncertainties in dose summation, and we verified the DIR accuracy before calculating doses to HR-CTV, IR-CTV, bladder, and rectum.

Chapter 3

Methods

3.1 Patient selection

Twenty locally advanced cervical cancer patients enrolled in the EMBRACE I (the intErnational study on MRI-guided BRAchytherapy in locally Advanced CErvical cancer) study were included in this analysis. ISVs were calculated for all twenty patients. Five patients were randomly selected to perform the dose summation using DIR. Patients were treated with EBRT to a dose of 45 Gy in 25 fractions and 4 fractions of HDR BT. EMBRACE I (2008 - 2015; NCT00920920) was a prospective observational study that aimed to benchmark MR guided adaptive BT in a multicenter setting. Inclusion/exclusion criteria are described in the EMBRACE protocol (link). The study has central Ethics Review Board (ERB) approval from the Medical University of Vienna.

3.2 Deformable image registration approaches and accuracy

DIR was performed by using Velocity software. All five patients had CT scans from EBRT treatment and 2 MRI image sets from the first (BT1) and third (BT3) BT fractions, corresponding to 2 different BT implants. Each BT implant was delivered over 2 BT fractions on consecutive days. The MR image of BT3 was chosen as a primary image, whereas the CT image of EBRT and the MR image of BT1 were secondary images. As a first step, rigid registration was used between the primary and secondary images to align the bony anatomy. Figure 4 illustrates the rigid registration between MR images of BT1 and BT3 for the rectum and bladder.

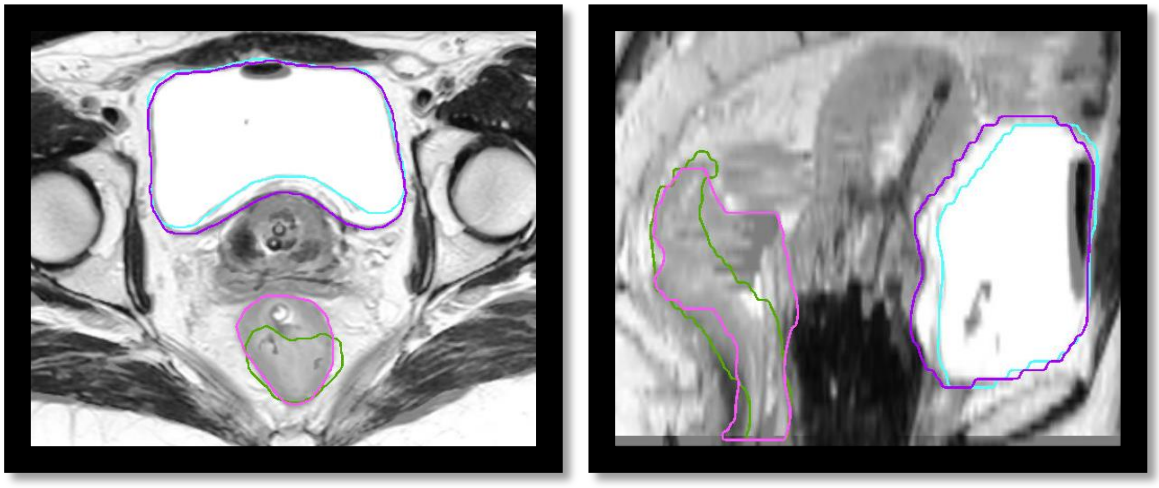

Figure 4. Rigid registration based on bony anatomy between BT1 and BT3 MR images. The rectum (pink (BT3) and green (BT1)) and bladder (purple (BT3) and cyan (BT1)) contours are displayed.

Between the BT3 and EBRT images, deformable multi-pass image registration was performed. Deformable multi-pass is a 3-pass DIR, where software runs image registration three times.

DIR between MR images of BT3 and BT1 was structure-based, and the registration metrics are improved compared to deformable multi-pass. Three different approaches to structure-based DIR were evaluated.

The first approach is DIR based on multiple structures. MR images were deformed based on the vagina, rectum, and bladder contours simultaneously. The second approach is DIR based on one structure, e.g., bladder, rectum, HR-CTV, and IR-CTV structures, using one structure at a time to guide registration. The third approach uses the density overwrite feature to perform DIR based on one structure. We deformed MR images based on HR-CTV, IR-CTV, bladder, and rectum structures separately by overwriting the structure's density value.

After evaluating the three approaches, the best approach was structure-based image registration with overwriting the structure density value to -1000 for the bladder and rectum separately. The evaluation results are provided in chapter 4.1. The DIR based on the one structure without overwriting the density value was performed to deform HR-CTV and IR-CTV, while the DIR

with density overwriting was the best for the bladder and rectum. DIR steps and selected approaches for each structure are shown in figure 5.

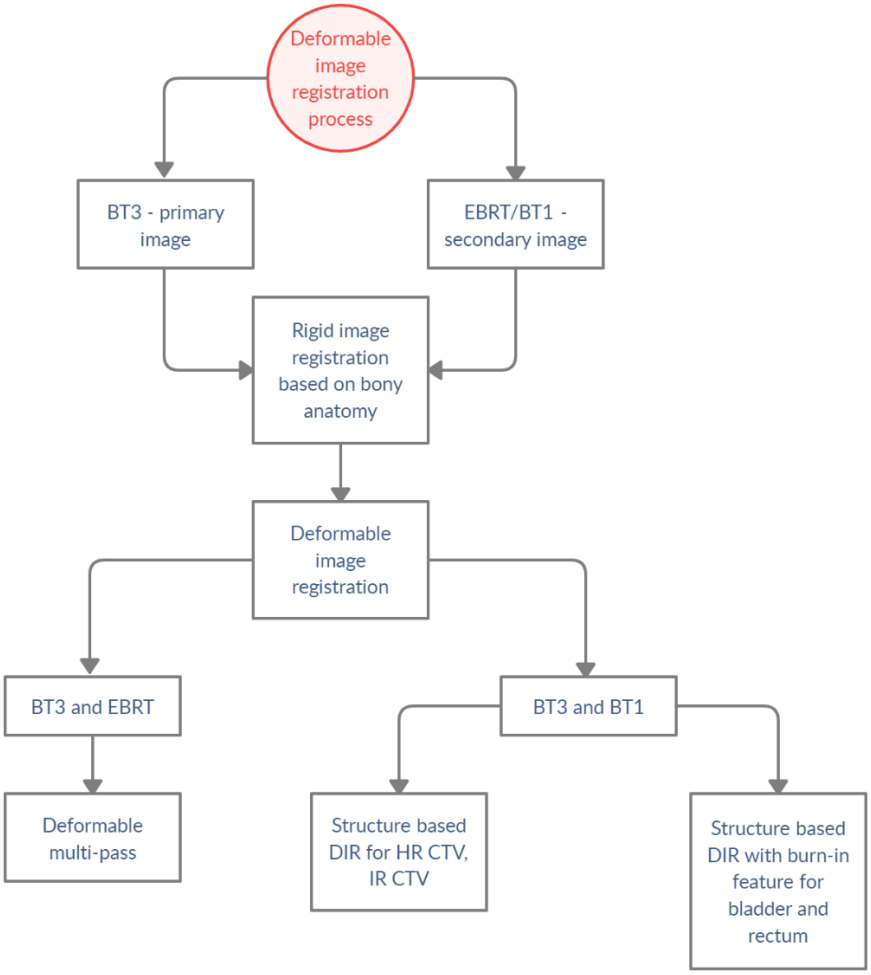

Figure 5. Deformable image registration steps and approaches for DIR.

DIR accuracy was analyzed by reporting the DSC, MDA, TRE and Jacobian described in chapter 2.1.5. DSC and MDA are obtained by measuring the Velocity software's conformality and surface distance metric. The Jacobians were acquired from the Velocity's deformable quality assurance tool.

3.3 Doses to HR-CTV, IR-CTV, bladder, and rectum

Accumulated equivalent doses to HR-CTV, IR-CTV, bladder, and rectum, were calculated using DA and DIR dose accumulation approaches.

For the DA approach, the first step was to read the physical dose from the DVH and subsequently to calculate the total equivalent dose with the direct addition method. Physical doses for HR-CTV and IR-CTV were collected from the Velocity software, whereas doses for bladder and rectum were collected from the Eclipse software. We could not obtain $D_{2\ cm^3}$ and $D_{0.1\ cm^3}$ in Velocity. Velocity does not provide the dose-volume histogram if the calculated dose does not fully cover the entire organ volume. As can be seen in figure 6, the dose calculation region of interest did not completely cover the bladder and rectum contours.

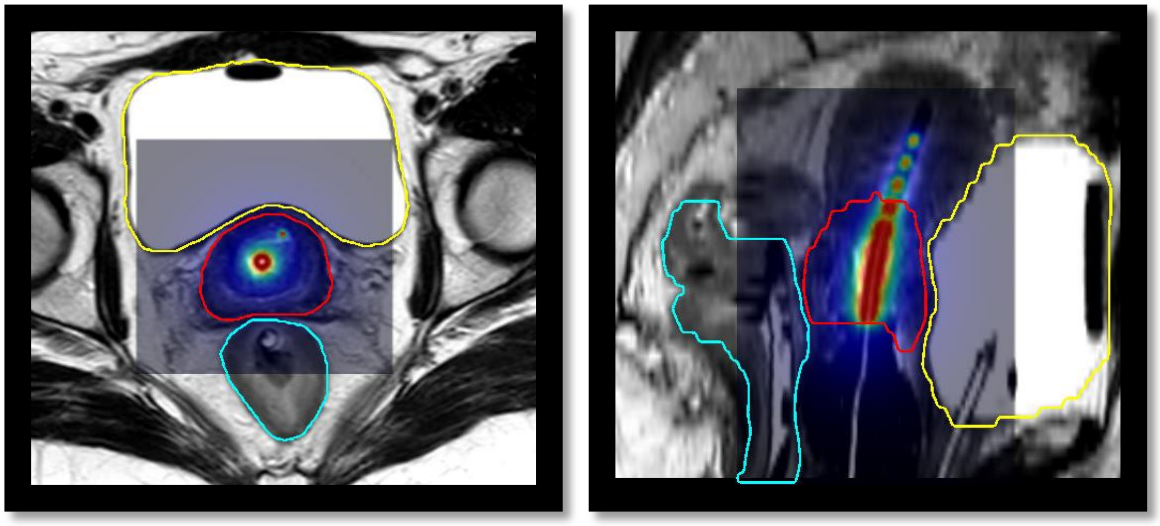

Figure 6. BT dose coverage in coulorwash for of the bladder and rectum contour. From this image we can see that dose fully covers the HR-CTV and IR-CTV, while the bladder and rectum are only half covered.

Collected physical doses were converted into EQD2 using Eq. (1). Calculated EQD2 doses are summed to obtain total equivalent doses in 2 Gy per fraction.

For the DIR dose summation approach, the total equivalent dose was calculated after performing a DIR. Before adding doses from EBRT and BT, the doses were converted to equivalent doses in Velocity. Two different resampled equivalent dose distributions were created for each treatment modality. The first resampled equivalent dose was created by converting the physical dose to the equivalent dose using the α/β=3 for the dose calculation of

OAR. The second resampled equivalent dose was created for the targets using $\alpha/\beta=10$. The BT1 and BT3 resampled equivalent doses were doubled since each plan was delivered twice.

Prior to the dose addition process, doses from EBRT and BT1 should be in the same DICOM frame of reference as the BT3 dose. To bring these dose distributions to the same DICOM frame of reference, rigid and DIRs are created between BT3 and EBRT and BT3 and BT1. Consequently, the dose distribution in the same DICOM frame of reference as EBRT/BT1 was chosen as the secondary image. DIR was used to create the resampled dose, which was in the same DICOM frame of reference as the BT3 dose. Finally, resampled doses from EBRT and BT1 were summed with the BT3 dose to get the total equivalent dose. A process map of the dose summation process is illustrated in figure 7.

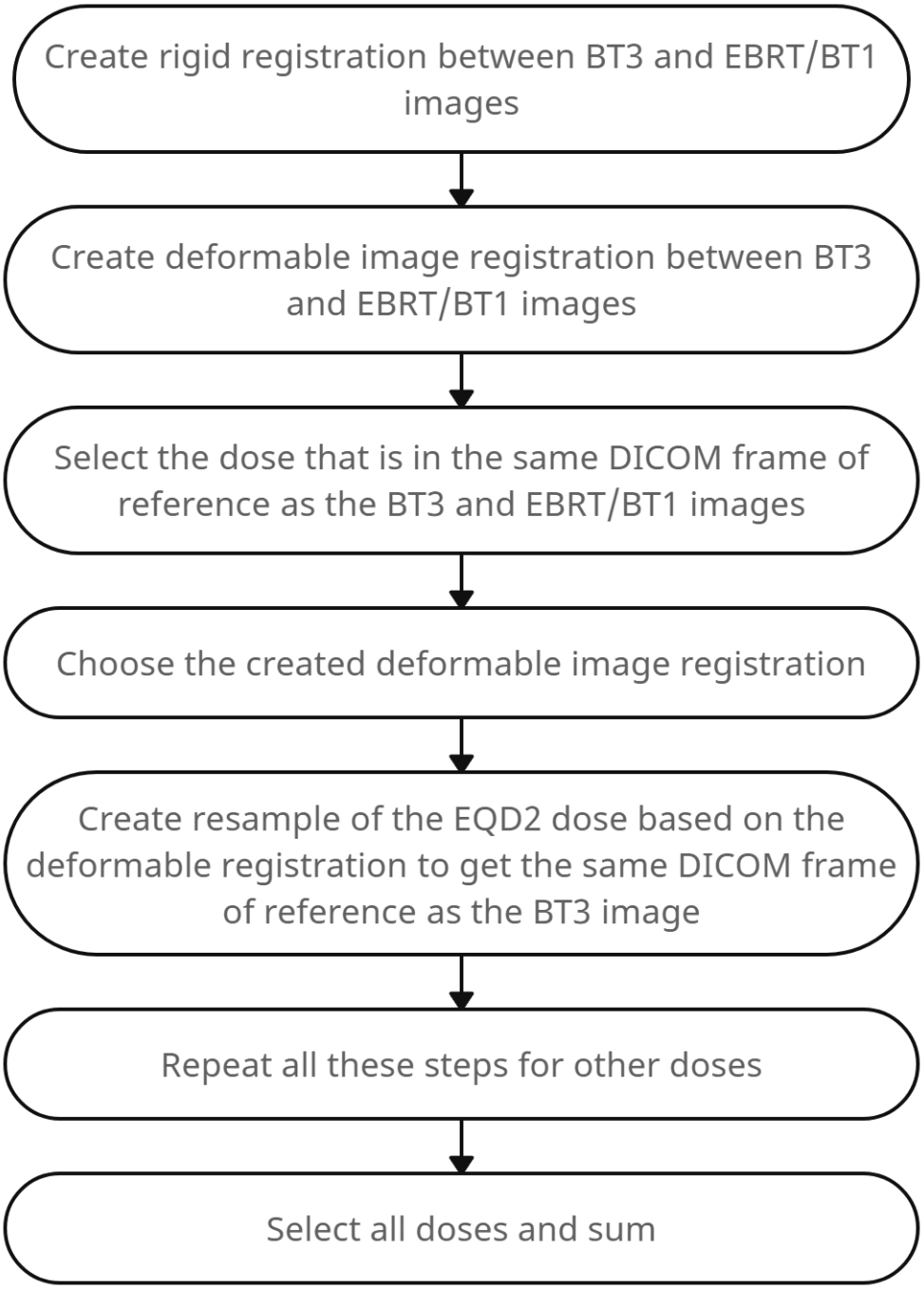

Figure 7. Dose summation process steps in Velocity.

Dose to the HR-CTV and IR-CTV are recorded and reported for D100%, D98%, D90%, and D50% (Figure 8).

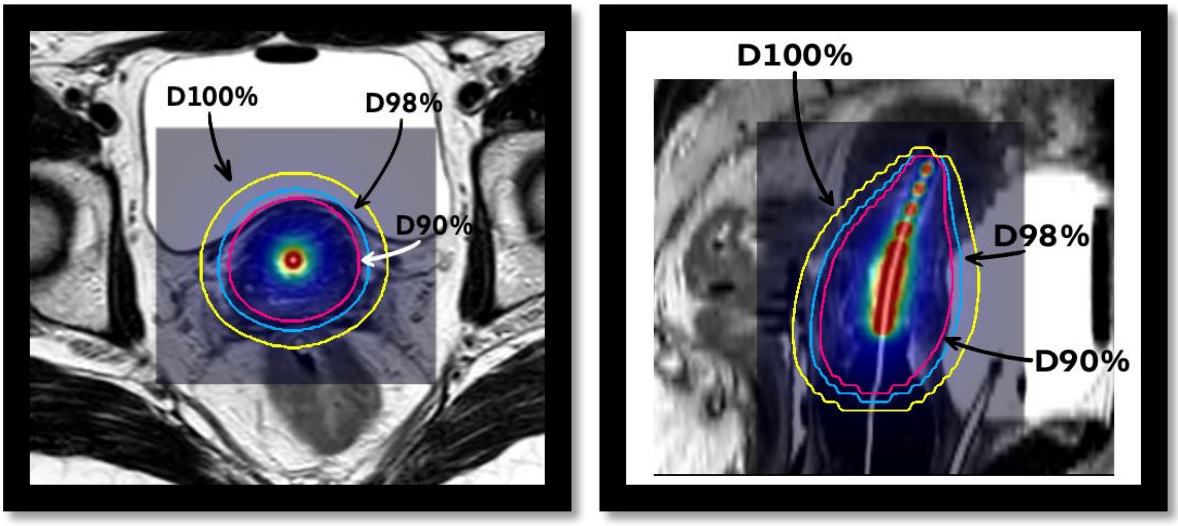

Figure 8. D100% (yellow), D98% (blue), D90% (red) isodose levels of HR-CTV.

Dose to the bladder and rectum are reported in $D_{2\ cm^3}$ and $D_{0.1\ cm^3}$ (Figure 9).

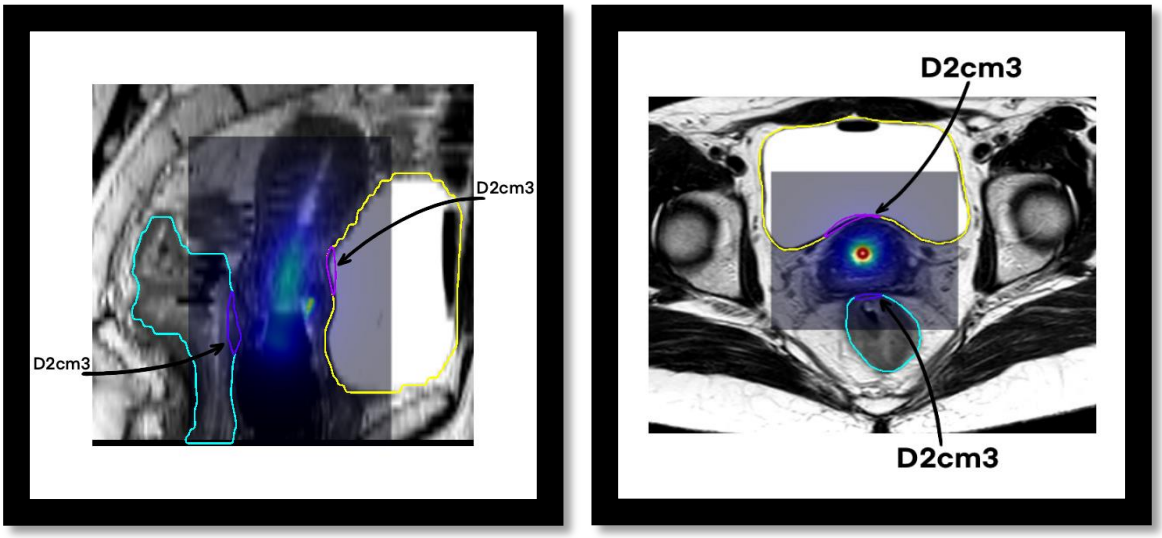

Figure 9. $D_{2\ cm^3}$ of the bladder (purple isodose line) and rectum (blue isodose line).

Doses obtained from the DIR method are compared with the direct addition method and reported in this study.

3.4 Isodose surface volumes

ISVs are calculated for twenty patients for three clinically relevant EQD2 dose levels: 85 Gy, 75 Gy and 60 Gy. ISVs are obtained with three different approaches for targets.

The first approach was to use the treatment planning system (TPS) to calculate the volumes encompassed by the isodose surface of the physical dose levels corresponding to 85, 75, 60 Gy EQD2 dose levels from BT1 and BT3 plan. The isodose dose levels were converted into structures for determination of the volume, and the average value of the measured volumes in BT1 and BT3 was calculated (Figure 10).

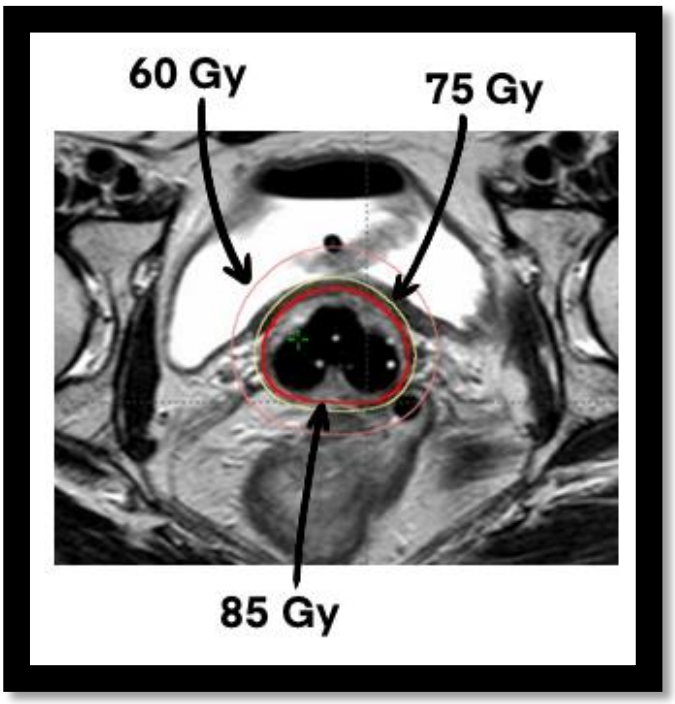

Figure 10. 85 Gy, 75 Gy, and 60 Gy EQD2 isodose surface volumes.

The second approach is the prediction of ISVs based on the Total Reference Air Kerma from BT. ISVs were calculated by equation:

$$ISV = 4965\left(\frac{TRAK}{d_{ref}}\right)^{\frac{3}{2}} + 170\left(\frac{TRAK}{d_{ref}}\right) - 1.5 \quad (8)$$

where,

TRAK – fractional Total Reference Air Kerma of the BT.

d_{ref} – the fractional physical BT dose corresponding to the total EBRT and BT EQD2 dose level. This calculation based on Nkiwane study [13]. Average values of BT1 and BT3 ISVs are calculated as cumulative ISV from EBRT and BT.

In the third approach, the ISVs were based on rigid image registration between BT3 and BT1/EBRT images in the Eclipse treatment planning system. Before image registration, the physical dose from EBRT and BT fractions was converted into EQD2 doses. The EQD2 conversion was performed using MIM software. The image registration between BT3 and BT1 was guided by matching the BT applicator.

The image registration between BT3 and EBRT was guided by bony anatomy. BT3 is the primary image, and BT1/EBRT were the secondary images. After the image registration, the dose summation was performed, and ISVs were calculated (Figure 11).

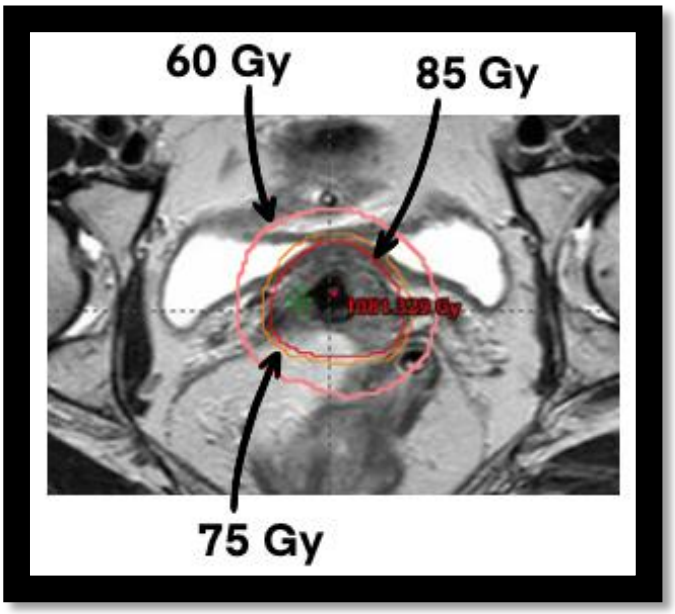

Figure 11. 85 Gy, 75 Gy, and 60 Gy isodose surface volumes were created after the dose summation of BT3, BT1 and EBRT doses.

The data resulting from the three methodologies are reported in Chapter 4.3.

Chapter 4

Results

4.1 Deformable image registration approaches

DIR based on multiple structures performed worse than the other two approaches. DSC for the bladder was 0.97, the rectum was 0.82, and the vagina was 0.91. MDA was 0.49 mm for bladder, 1.87 mm for rectum, and 1.02 mm for vagina. Organ alignments of DIR based on multiple structures are shown in figure 12.

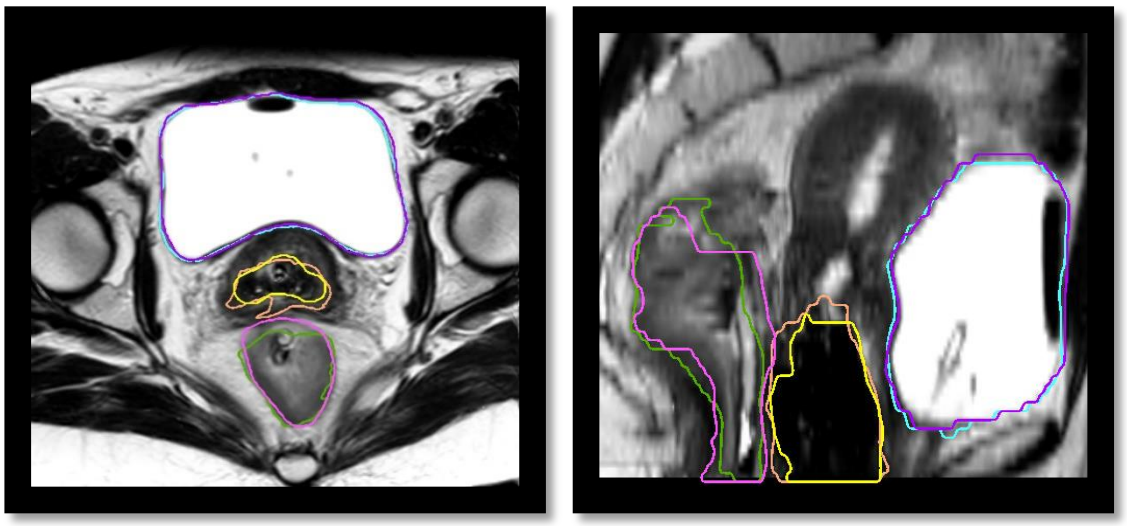

Figure 12. Deformable image registration based simultaneously on matching the vagina (yellow and orange), rectum (pink and green), and bladder (purple and cyan) contours.

DIR based on a single structure approach performed better than DIR based on multiple structures, as shown in the rectum contours comparison from figure 12 and figure 13. DSC for the rectum was increased from 0.82 to 0.85, while MDA was decreased from 1.87 mm to 1.57 mm.

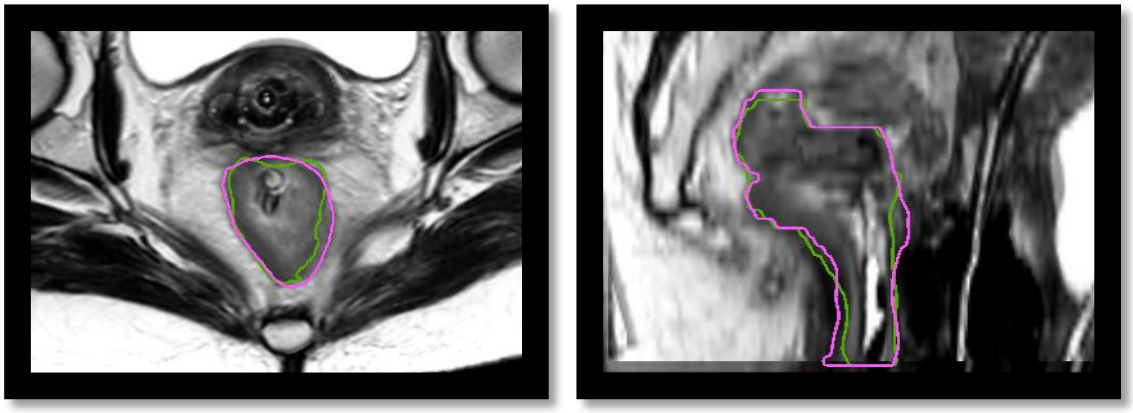

Figure 13. Deformable image registration based on the rectum contour.

DIR based on a single structure with a density overwrite feature demonstrated the best alignment. The DSC increased to 0.92, and MDA decreased to 0.77 mm. The DIR with density overwrites feature based on rectum contour is illustrated in figure 14.

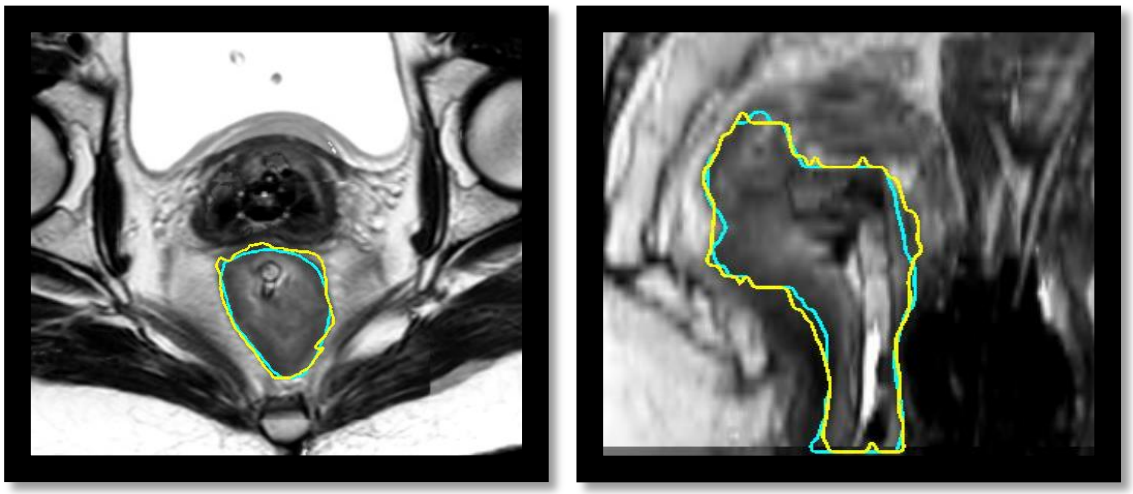

Figure 14. Deformable image registration based on the rectum with the density overwrite feature.

4.2 Deformable image registration accuracy

We evaluated the DSC, MDA, TRE, and Jacobian registration metrics to validate DIR accuracy. Table 1 shows the DSC, MDA and Jacobian mean values for bladder, rectum, HR-CTV, and IR-CTV.

Table 1. Average image registration metrics for bladder, rectum, HR-CTV, and IR-CTV.

	Bladder	Rectum	HR CTV	IR CTV
DSC	0.93 (0.90–0.98)	0.88 (0.81–0.92)	0.82 (0.75–0.88)	0.88 (0.83–0.92)
MDA (mm)	0.70 (0.35–1.02)	1.11 (0.62–2.25)	1.37 (0.71–2.45)	1.74 (1.02–2.70)
Jacobian	1.33 (-4.49–10.96)	1.22 (-0.29–12.22)	1.02 (-0.15–3.39)	0.93 (-0.87–2.67)

The DIR had a mean DSC of 0.93 for bladder, 0.88 for rectum, 0.82 for HR-CTV, and 0.88 for IR-CTV. DSC measured in Velocity gave results higher than 0.8 as recommended in TG-132. The distribution of DSC values for bladder, rectum, HR-CTV, and IR-CTV structures are shown in figure 15.

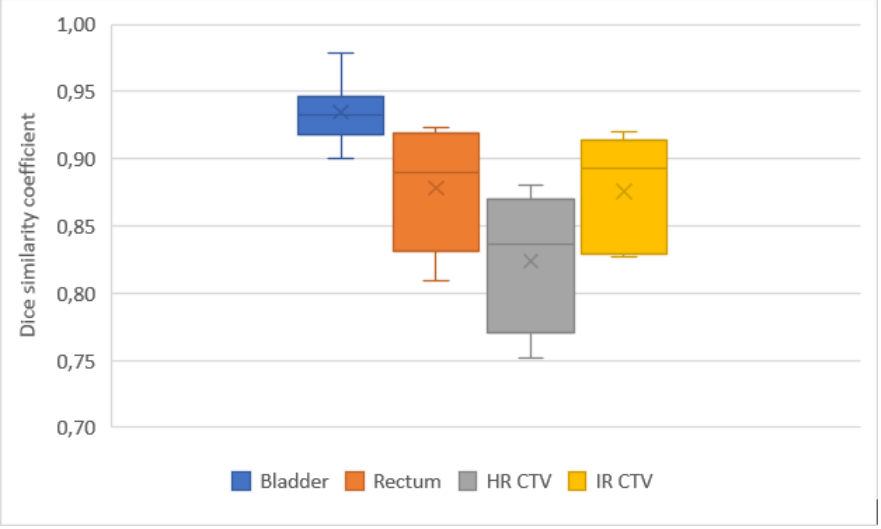

Figure 15. The dice similarity coefficients variations for bladder, rectum, HR-CTV, and IR-CTV structures over 5 patients.

The average value of the MDA is 0.70 mm for bladder, 1.11 mm for rectum, 1.37 mm for HR-CTV, and 1.74 mm for IR-CTV. The values of the MDA for each structure are presented in figure 16.

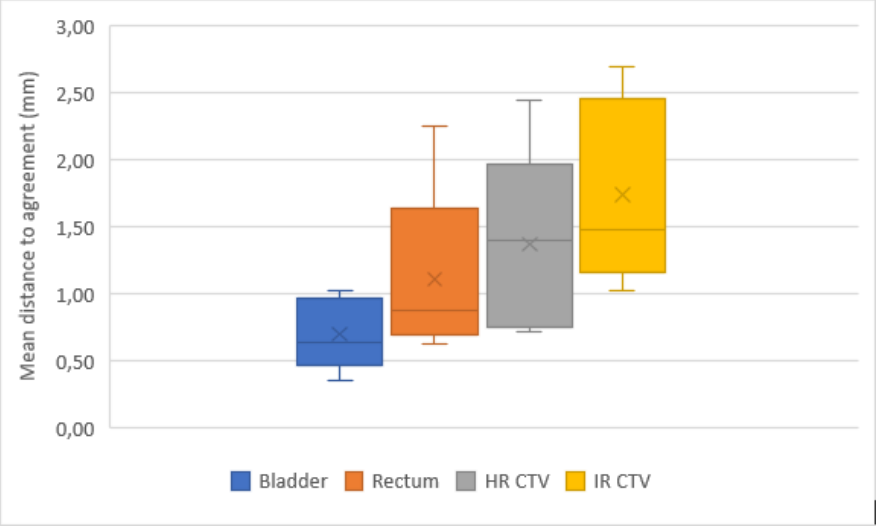

Figure 16. The mean distance to agreement distribution for bladder, rectum, HR CTV, and IR CTV over 5 patients.

Jacobian ranges between -4.5 and 11.00 for bladder, -0.3 and 12.2 for rectum, -0.1 and 3.4 for HR-CTV, and -0.9 and 2.7 for IR-CTV. All image registrations had negative Jacobians, at least for one structure. However, these negative Jacobian values represented small volumes of the structure. 2.3% of the bladder, 0.2% of the rectum, 0.4% of the HR-CTV, and 1.7% of the IR-CTV have negative Jacobian values. The Jacobian maps of all image registrations were studied to find the volume with nonphysical deformations. Figure 17 shows Jacobian maps for the image registrations with the largest nonphysical motions for each structure.

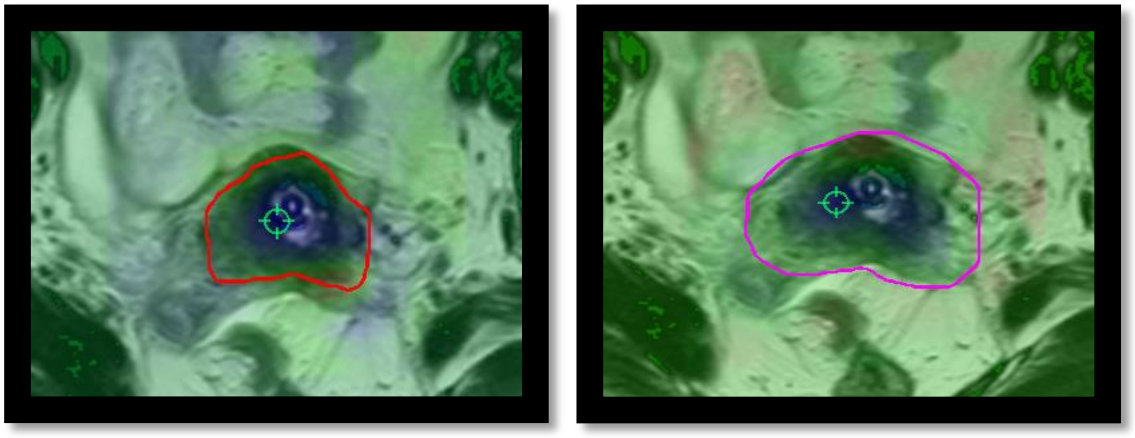

A. HR CTV

B. IR CTV

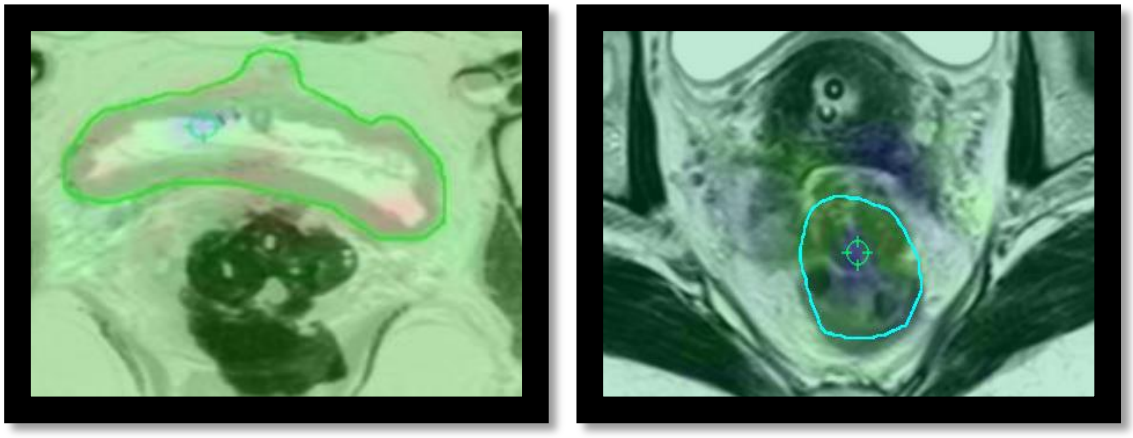

C. Bladder D. Rectum

Figure 17. The Jacobian maps of deformable image registrations with largest volume of negative Jacobians. Green color inside of the structure shows positive Jacobian, while dark blue color shows negative Jacobian.

The negative Jacobian is mainly in the region of applicator for HR-CTV and IR-CTV and in the middle of the structure for the bladder and rectum. Negative Jacobian should not affect the reporting doses. Figure 17 A shows the only DIR with the negative Jacobian for the HR-CTV structure. The minimum Jacobian value is -0.15, covering 1.73% of the HR-CTV structure volume. Figure 17 B illustrates the DIR based on IR-CTV with the most extensive jumping and folding voxels among all structures. The largest negative Jacobian volume covers 6.49% of IR-CTV structure volume. Figure 17 C shows the DIR with the highest negative Jacobian value, which equals -4.49 and covers 3.34% of the bladder volume. Figure 17 D illustrates the DIR with a negative value of -0.76, covering only 1.03% of rectum volume.

The mean Jacobian values showed that the vast majority of the percentage of structure volumes, i.e., 98.66% of the bladder, 99.79% of the rectum, 99.65% of the HR CTV, and 98.28% of the IR CTV structure volumes had positive Jacobian values. The figure 18 presents the distributions of minimum, maximum, and mean Jacobian values.

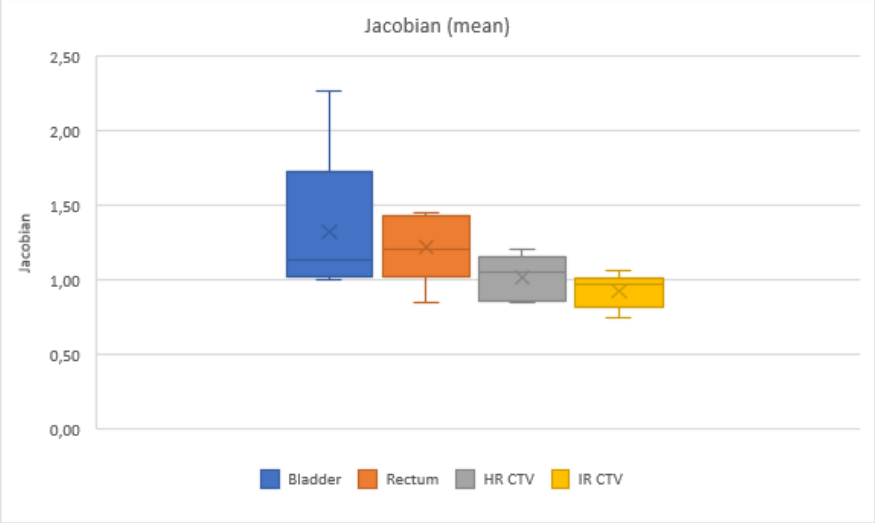

Figure 18. The variabilities of minimum, maximum, and mean Jacobians for each structure.

4.2 Doses to HR-CTV, IR-CTV, bladder, and rectum from the DIR for cervical cancer

Mean cumulative dose parameters for HR-CTV and IR-CTV calculated using the DA method are illustrated in figure 19. The DA of DVH parameters resulted in an average HR-CTV dose of 69.13 Gy for D100%, 78.72 Gy for D98%, 90.10 Gy for D90%, and 134.44 Gy for D50%. Average IR-CTV D100% was 56.42 Gy and D98% was 61.38 Gy.

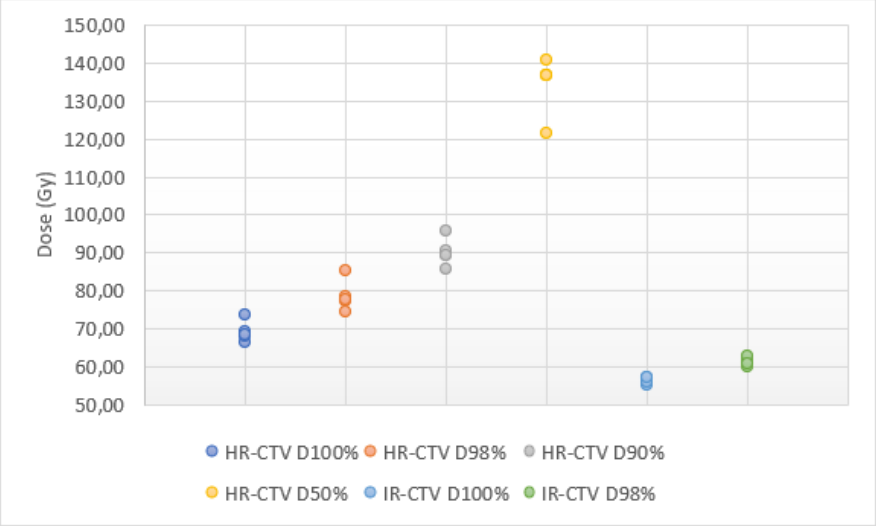

Figure 19. The mean variation of doses computed with direct addition method for HR-CTV and IR-CTV over the 5 patients.

The comparison of total EQD2 doses from the DA method and accumulated dose using DIR is shown in table 2 for HR-CTV and table 3 for IR-CTV.

Table 2. The comparison between DA and DIR for HR-CTV.

Methods		HR CTV			
		D100% (Gy)	D98% (Gy)	D90% (Gy)	D50% (Gy)
DA	mean	69.13	78.72	90.10	134.44
	range	66.4–73.50	74.52–85.50	85.63–95.69	121.59–140.77
DIR	mean	70.09	80.14	91.48	136.79
	range	63.47–76.91	75.30–87.51	84.30–97.63	117.88–146.09
DA-DIR (Gy)	mean	-0.96	-1.42	-1.38	-2.35
DA-DIR (%)	mean	-1.24	-1.75	-1,47	-1.59

Table 3. The comparison between DA and DIR for IR-CTV.

Methods		IR CTV	
		D100% (Gy)	D98% (Gy)
DA	mean	56.42	61.38
	range	55.17–57.23	59.87–62.79
DIR	mean	57.67	62.59
	range	55.53–60.72	60.51–65.40
DA-DIR (Gy)	mean	-1.25	-1,21
DA-DIR (%)	mean	-2.15	-1.93

The comparison of DA and DIR showed that the HR-CTV doses calculated by the DIR were 1.2% higher for D90%, 1.8% higher for D98%, 1.5% higher for D90%, and 1.6% higher for D50% than the DA method. A similar trend was seen when comparing DA and DIR for IR-

CTV. The cumulative dose calculated by DIR for IR-CTV for D100% was 2.15% greater than the DA method, whereas the cumulative dose of D98% was 1.93% greater. The difference (%) variation over five patients for HR-CTV and IR-CTV is presented in figure 20.

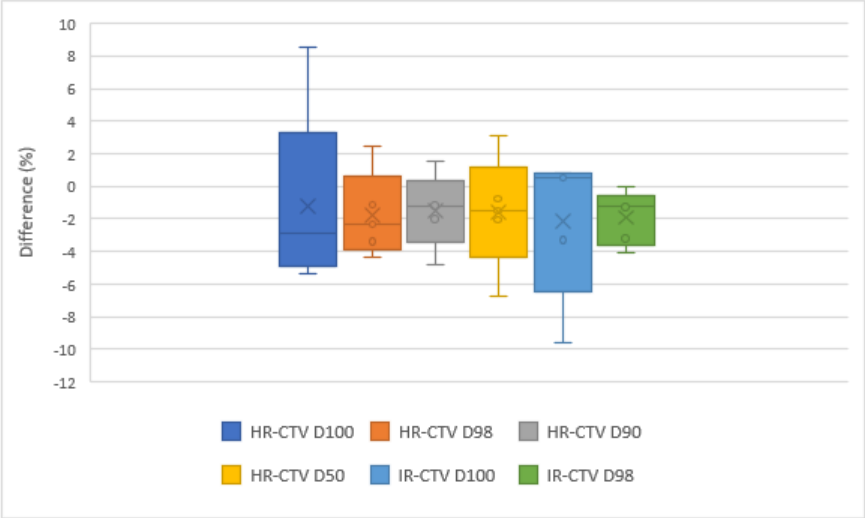

Figure 20. DA and DIR difference in percent for HR-CTV and IR-CTV for over 5 patients.

Figure 21 displays the mean total dose variation of bladder and rectum calculated with a DA method for over 5 patients. The $D_{2\ cm^3}$ and $D_{0.1\ cm^3}$ calculated by the DA method were 85.22 Gy and 106.88 Gy for the bladder, and 61.41 Gy and 73.45 Gy for the rectum, respectively.

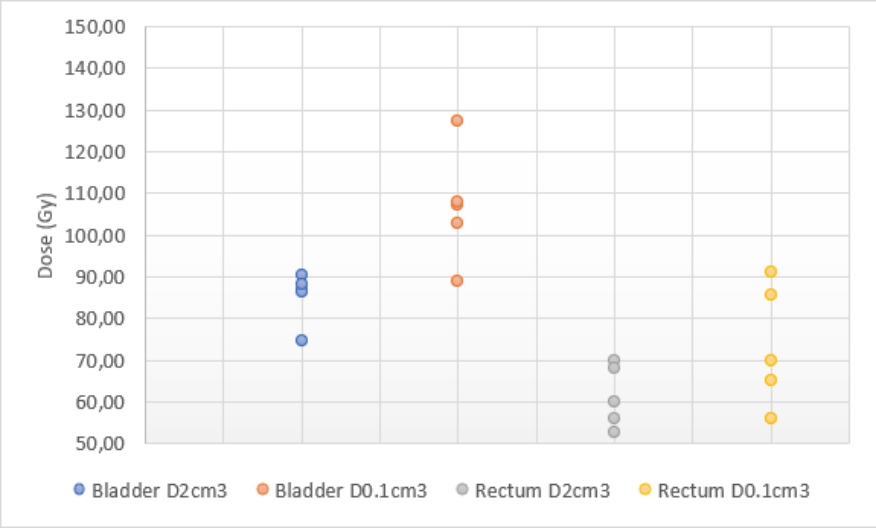

Figure 21. The mean total dose variation computed by DA method for bladder and rectum.

The calculated total doses from the DA approach and doses obtained from the DIR for bladder and rectum are compared and illustrated in table 4.

Table 4. The comparison of DA and DIR for bladder and rectum.

Methods		Bladder		Rectum	
		$D_{2\ cm^3}$	$D_{0.1\ cm^3}$	$D_{2\ cm^3}$	$D_{0.1\ cm^3}$
DA	mean	85.22	106.88	61.41	73.45
	range	74.58–90.44	89.04–127.47	52.67–69.96	55.86–91.16
DIR	mean	79.37	99.72	61.40	71.87
	range	72.43–89.77	87.94–114.56	52.41–69.12	54.99–85.92
DA-DIR (Gy)	mean	5.85	7.17	0.01	1,57
DA-DIR (%)	Mean	7.14	6.72	0.01	1.97

The accumulated dose of bladder $D_{2\ cm^3}$ calculated by DIR was lower by 7.14%, and the $D_{0.1\ cm^3}$ was lower by 6.72% than the DA method. The total dose difference between DIR and DA for rectum was 0.01% for $D_{2\ cm^3}$ and 1.97% for $D_{0.1\ cm^3}$. Figure 22 illustrates the difference (%) variation for the bladder and rectum for over 5 patients.

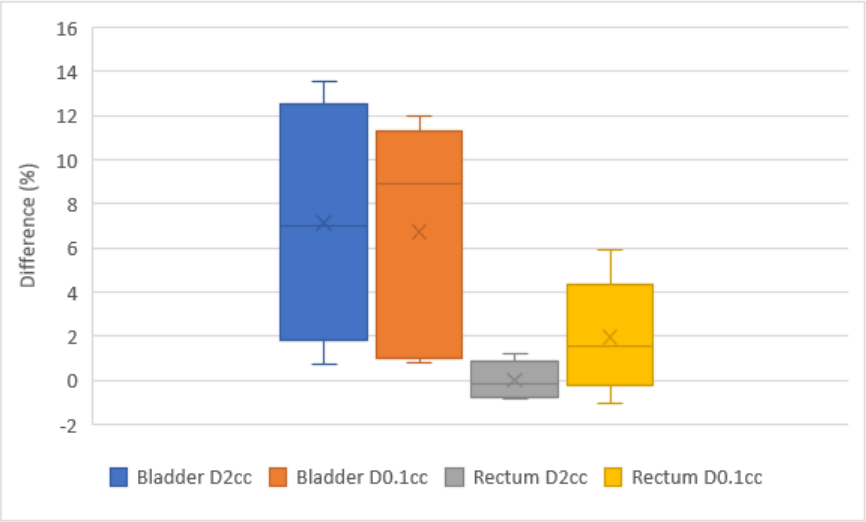

Figure 22. DA and DIR difference in percent for bladder and rectum

4.3 Isodose surface volumes

The average ISVs for the clinically relevant 85 Gy, 75 Gy, and 60 Gy EQD2 doses obtained with three different methods are illustrated in table 5.

Table 5. The ISV for 85Gy, 75 Gy, and 60 Gy EQD2 doses were calculated by predictive model (ISV_{pred}), read from physical dose in the TPS (ISV_{TPS}), and measured from rigid registration based on applicator methods.

	ISV_{pred} (cm^3)	ISV_{TPS} (cm^3)	ISV_{reg} (cm^3)
V85Gy	71.0	68.0	71.4
V75Gy	95.4	92.5	97.3
V60Gy	201.4	195.8	204.9

The distributions of volumes for each EQD2 dose and method are provided in Fig 23.

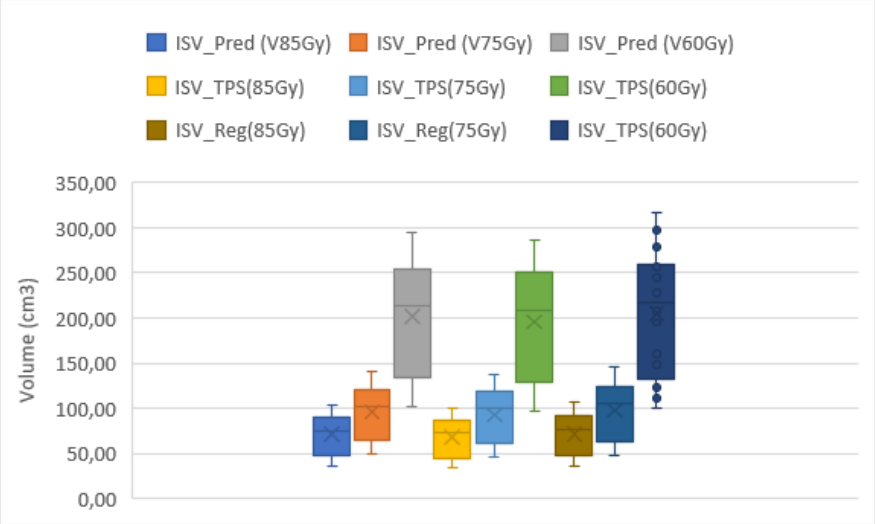

Figure 23. The ISVs distribution of 85 Gy, 75 Gy, and 60 Gy EQD2 doses were calculated based on a predictive model [13] (ISV_{pred}), derived from the TPS by measurement of the volume encompassed by physical isodoses corresponding to cumulative EQD2 levels of 85 Gy, 75 Gy, and 60 Gy (ISV_{TPS}), and determined from rigid image registration based on applicator matching.

The average percent difference between the ISV_{TPS} and ISV_{pred} was – 4.40% ± 1.92 % for 85 Gy, -3.29% ± 1.62% for 75 Gy, and -3.04% ± 1.25% for 60 Gy. Figure 24 provides the % difference between ISV_{TPS} and ISV_{pred}.

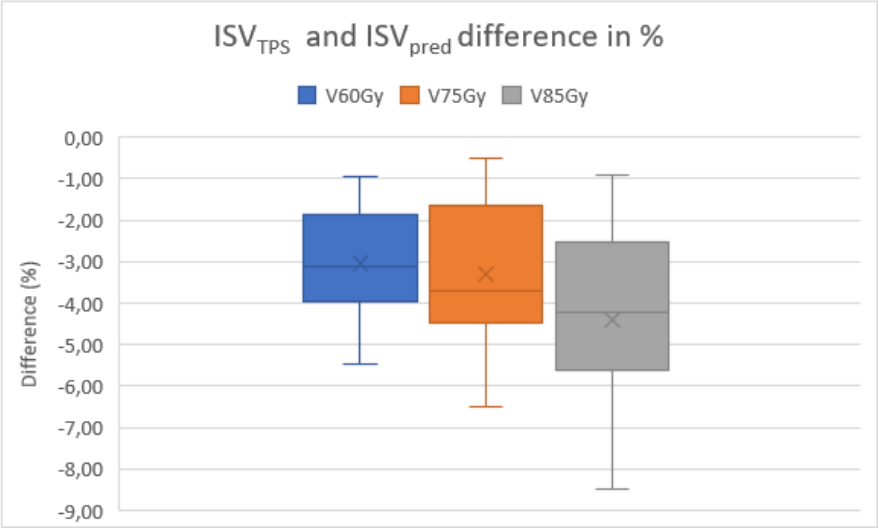

Figure 24. Percent differences between ISV_{TPS} and ISV_{pred} encompassed by 85 Gy, 75 Gy, and 65 Gy EQD2.

The mean percent difference between the ISV_{TPS} and ISV_{reg} was – 4.68% ± 1.63 % for 85 Gy, -4.77% ± 1.58 % for 75 Gy, and -4.21% ± 2.16% for 60 Gy. The distribution of isodose surface volumes for 85 Gy, 75 Gy, and 60 Gy are shown in figure 25.

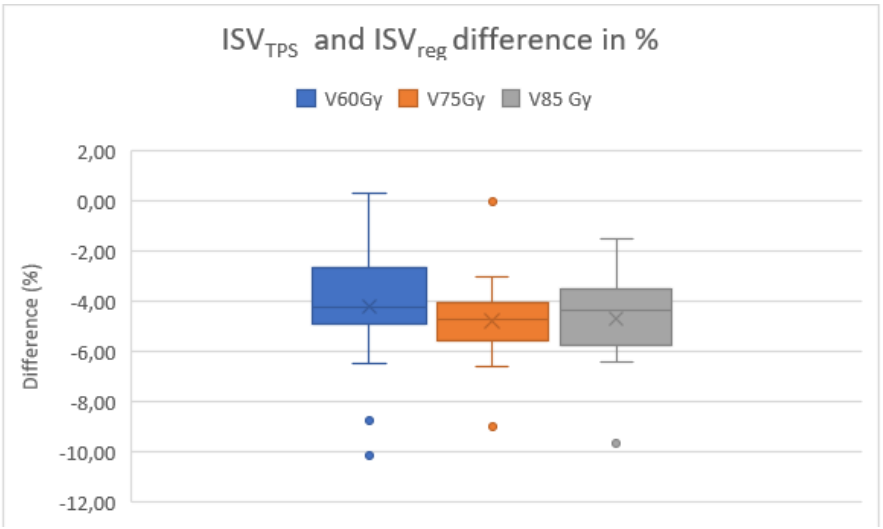

Figure 25. Percent differences between ISV_{TPS} and ISV_{reg} encompassed by 85 Gy, 75 Gy, and 65 Gy EQD2.

The average difference between ISV_{reg} and ISV_{pred} was 0.28% ± 2.99% for 85 Gy, 1.48% ± 2.70% for 75 Gy, 1.16% ± 2.80% for 60 Gy. The difference of isodose surface volumes for 85 Gy, 75 Gy, and 60 Gy are illustrated in figure 26.

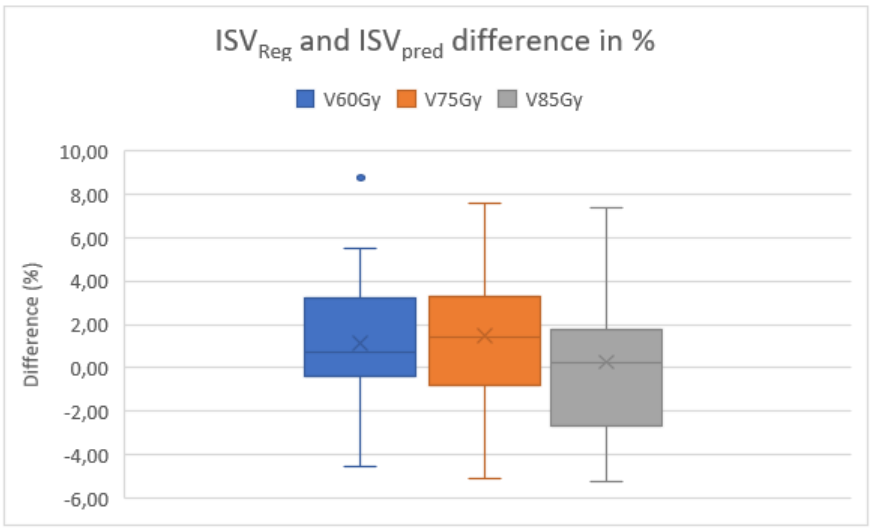

Figure 26. Percent differences between ISV_{TPS} and ISV_{pred} encompassed by 85 Gy, 75 Gy, and 65 Gy EQD2.

Chapter 5

Discussion

5.1 Deformable image registration accuracy

Current clinical practice is limited with respect to OAR dose reporting and uses (1) DA method at high dose levels in the region of the BT boost, e.g., $D_{2\ cm^3}$ and $D_{0.1\ cm^3}$, from EBRT + BT in EQD2, assuming the worst-case scenario; (2) intermediate dose levels evaluation from EBRT only. In this study we investigated the use of DIR for dose summation between EBRT and BT with the aim to improve on the limitations of the current approaches for dose reporting based on the simple DA method.

The DIR was performed in five LACC patients and registration accuracy was determined in this study. According to the TG-132, DSC should be higher than 0.80, MDA and TRE should

be 2-3 mm, and should have only positive Jacobians. The DIR accuracy evaluation demonstrated that all deformed images have DSC and MDA in the tolerance range. Negative Jacobians have primarily occurred in the center of the registered structure. Comparing the registrations metrics acquired from the registration of OAR and target structures, OAR has better DSC and MDA than clinical target volumes. There are 2 considerations that will explain this observation. The first aspect is the difference between approaches on DIR used for OAR and targets. The DIR based on a single structure with the burn-in feature, which was used to perform DIR for bladder and rectum, has better alignment than DIR based on the single structure used for HR-CTV and IR-CTV, because it overwrites voxel intensity to the same value. However, by studying the range of Jacobians, we can determine that the DIR based on a single structure with a burn-in feature has a wide range of Jacobians. This shows that the structure alignment (DSC and MDA) is improved, but it also raises the number of nonphysical deformations (negative Jacobian) inside the hollow organ. The second aspect is factors that affect the shape and position of structures. The bladder and rectum are mainly affected by their fillings and have less organ motions than the cervix. In contrast, HR-CTV and IR-CTV are affected by the applicator insertion, tumor shrinkage, and by rectum filling. The position of the cervix-uterus changes dramatically with the insertion of the applicator.

The DIR of the organs at risk could be significantly improved if we keep organ filling consistent, e.g., full or empty throughout the treatment. The evaluation of DIR based on bladder showed that full bladders have better accuracy and alignment than empty bladders. This could be seen in figure 27, where two bladders with different fillings are shown prior to DIR and after DIR.

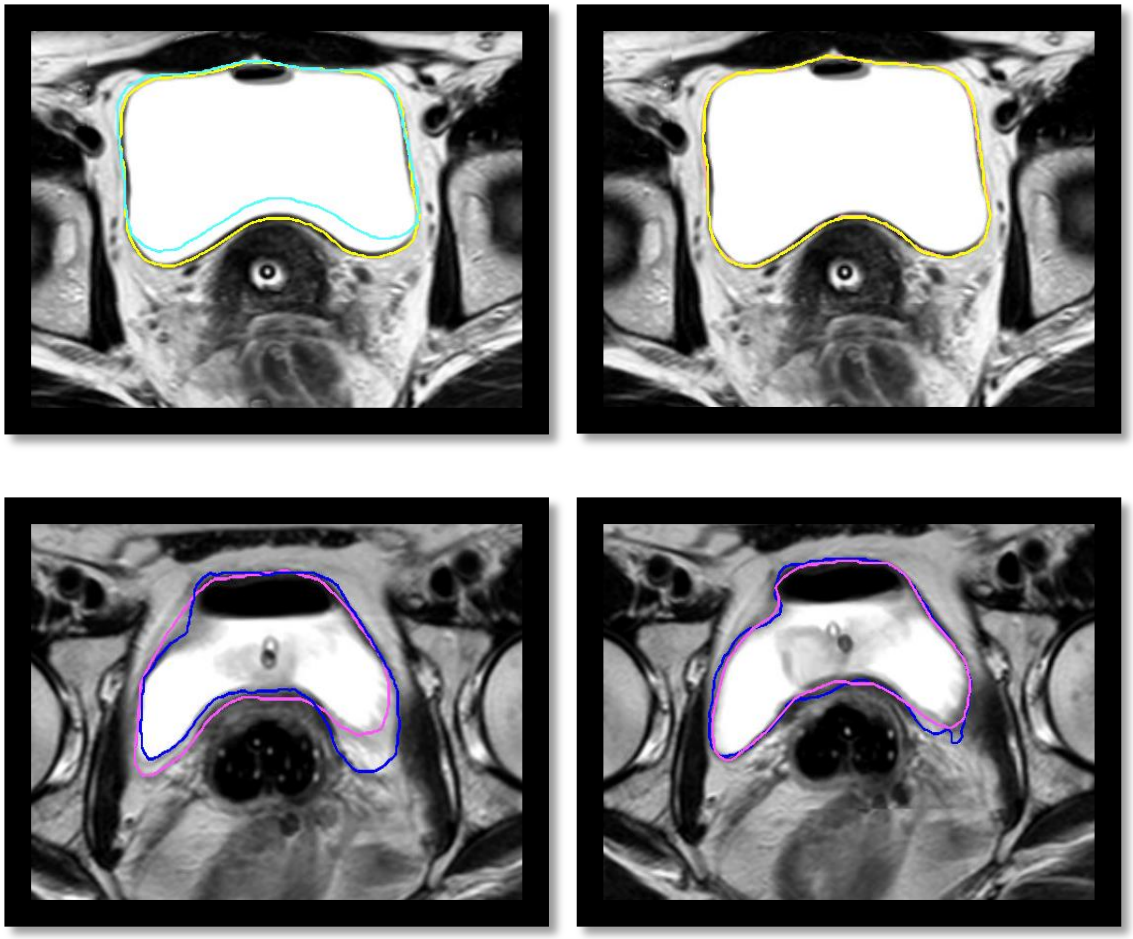

Figure 27. Bladders with two different fillings.

However, the full bladder could get a higher dose because it will be closer to the HR-CTV. Gerber et al. [19] reported that the ratios and absolute differences of the whole organ to wall doses for bladder were significantly higher for full bladder patients. Moreover, Zakariaee et al. [20] suggested that varying the bladder filling regimen could reduce urinary toxicity by avoiding overlapping hotspots.

The evaluation of registration metrics was limited by the difficulty of identifying homologous points in the images to measure TRE.

5.2 Doses to HR-CTV, IR-CTV, bladder, and rectum from the DIR for cervical cancer

Abe et al. [21] discussed that DA of $D_{2\ cm^3}$ is an overestimation for OAR, whereas the D90% of HR-CTV is typically an underestimation.

However, in this study, the DA and DIR comparison revealed that the percent difference between doses to the HR-CTV and IR-CTV was higher than 2% with the DIR as compared to the DA method. The bladder doses were slightly overestimated, which means that DVH hotspots were only partly overlapping. The difference between accumulated doses of the rectum $D_{2\ cm^3}$ was 0.01%, which indicates that hotspots fully overlapped, and the worst-case scenario appeared to be a good method for reporting hotspots in this OAR. However, prudent judgment must be taken when analyzing the accumulated dose from DIR. The overall results showed that the DIR gave a higher dose than DA due to the uncertainties caused by complications of performing DIR.

5.3 Isodose surface volumes

V60 Gy reference volume, derived from the half product of height, width, and thickness (HWT) [1,22], has been used in the past to compare treatment schedules and to investigate correlation with doses to OARs and morbidity (e.g., scattergram plots of HWT against cumulated rectal mean were used to differentiate zones of rectal complications) [1,23-27]. However, the V60 Gy reference volume has not become widespread in the international community for reporting purposes [28].

Based on the idea of the ICRU 38 Report 60 Gy reference volume, the ICRU Report 89 introduced the concept of isodose surface volumes (ISVs) as the volumes encompassed by clinically relevant cumulative dose levels (e.g., 60 Gy, 75 Gy and 85 Gy EQD2) and referring to both target and OARs [7]. Since ISVs are independent of contoured target volumes and

related to the dwell times, source strength and implant geometry, these volumes can therefore be regarded as surrogates of treatment intensity. As "an isodose surface volume should be linked to a dose that is judged as representative for a certain clinical effect" [9], the ISVs may add to the understanding of risk factors for treatment related toxicity and local disease failure in addition to DVH parameters for OAR and target volumes.

It has been demonstrated that DVH parameters for CTV_{HR}, GTV_{res} and CTV_{IR} (e.g., $D_{98\%}$, $D_{90\%}$) correlate with local control [29], however, these doses do not directly reflect the overall intensity of the treatment. On the contrary, CTV_{HR} dose is generally higher in patients with small tumours and small ISVs [30]. For advanced IC/IS IGABT, Point A cannot be used for dose reporting due to proximity of needles. Therefore, the long-term anchorage to previous clinical practice has been missing critically. However, the ISVs can be used to make the connection to previous clinical practice and to compare treatments within and across different institutions and EBRT/BT fractionation schedules.

The ISVs distribution of 85 Gy, 75 Gy, and 60 Gy EQD2 doses were calculated based on a predictive model [13] (ISV_{pred}), derived from the TPS by measurement of the volume encompassed by physical isodoses corresponding to cumulative EQD2 levels (ISV_{TPS}), and determined from rigid image registration based on applicator matching.

The ISVs extracted from the treatment planning system (ISV_{TPS}) had the smallest volume and varied by roughly 5% for 85 Gy as compared to the TRAK-based predictive model (ISV_{Pred}) and based on rigid registration (ISV_{Reg}) techniques. This difference decreases as the dose lowers. Nkiwane et al. [13] demonstrated that TRAK could be used to calculate isodose surface volumes with good precision. The difference between ISV_{reg} and ISV_{pred} was negligible. Therefore, this study showed that ISV_{TPS}, ISV_{pred}, and ISV_{Reg} are in very good agreement.

ICRU Report 89 [7] recommends the use of ISVs as advanced tools (level 2 reporting) for reporting the dose in BT for cervical cancer. To this end, the ISVs are extracted directly from the TPS using our first method of calculation, ISV_{TPS}. On the other hand, TRAK has been used for reporting BT treatments for a long time, being recommended by ICRU report 38 [31]. Our second method of calculation, ISV_{pred}, uses TRAK and a predictive model to calculate the ISVs. This method is used for deriving the ISVs in clinical studies, where only TRAK is reported by the enrolling centres. Finally, our third determined ISVs based on rigid registration between EBRT and BT images. This method was deemed to be the most accurate methodology. In this study we showed the difference between the three methods when calculating ISVs is not clinically significant, and therefore methods ISV_{pred} and ISV_{TPS} are safe to be used for reporting this treatment parameter.

Chapter 6

Conclusion

Overall, DIR showed good accuracy. The DIR provided a mean dice similarity coefficient of 0.93 for bladder, 0.88 for rectum, 0.82 for HR CTV, and 0.88 for IR CTV. According to the TG-132 recommendations, DSC should be higher than 0.8. The mean distance to agreement varied between 0.35 and 1.02 for bladder, 0.62 and 2.25 for rectum, 0.71 and 2.45 for HR CTV, and 1.02 and 2.70 for IR CTV. TG-132 recommended that MDA should be less than 2-3 mm. The DSC and MDA passed the acceptable threshold recommended by TG-132. The comparison of DA and DIR methods gave a 2% higher dose of HR-CTV and IR-CTV doses computed by the DIR method. The bladder doses were slightly overestimated by DA method due to only partly overlapping hot spots. The difference in rectum $D_{2\,cm^3}$ between the two methods showed dose differences of 0.01%, indicating that hotspots overlap.

In conclusion, we do not recommend using the DIR method in the clinic which is also in line with the conclusion of Swamidas et al review [8]. This statement was made based on the challenges of performing DIR, mentioned in chapter 2.5, which leads to uncertainties in the dose calculation process. The most common example is the presence of negative Jacobian in the deformed image, which means an error in DIR and ideally should not exist. Although the different metrics to quantify DIR accuracy were meeting the TG-132 recommendations, the implementation of DIR in the clinical practice, based on single OAR structure-based approach requires multiple DIR for different OARs. This process is nevertheless lengthy, complex and not realistic, due to the time constraints when planning BT cases. Moreover, the DIR is commonly used for rectum and bladder, whereas there are only a few reports for highly mobile organs such as bowel and sigmoid [8]. Furthermore, dose addition for target doses, with shrinking tumours is not understood, and could result in large uncertainties. In this study, the

mean doses of the HR-CTV and IR-CTV were higher in DIR than DA due to the uncertainties which could be taken as an example of consequences of challenges of DIR.

ISV_{TPS} and ISV_{Pred} could be used to assess the isodose surface volumes with good precision.

References:

1. Sung H, Ferlay J, Siegel RL, Laversanne M, Soerjomataram I, Jemal A, Bray F. Global Cancer Statistics 2020: GLOBOCAN Estimates of Incidence and Mortality Worldwide for 36 Cancers in 185 Countries. CA Cancer J Clin. 2021 May;71(3):209-249. doi: 10.3322/caac.21660. Epub 2021 Feb 4. PMID: 33538338.
2. Potter R, Haie-Meder C, Van Limbergen E et al (2006) Recommendations from gynaecological (GYN) GEC ESTRO working group (II): concepts and terms in 3D image-based treatment planning in cervix cancer brachytherapy-3D dose volume parameters and aspects of 3D image-based anatomy, radiation physics, radiobiology. Radiother Oncol 78(1):67–77. https://doi.org/10.1016/j.radonc.2005.11.014 - DOI - PubMed
3. Rigaud B, Klopp A, Vedam S, et al. Deformable image registration for dose mapping between external beam radiotherapy and brachytherapy images of cervical cancer. Phys Med Biol 2019; 64:115023.
4. ICRU: ICRU Report 50 - prescribing, recording, and reporting photon beam therapy. International Commission on Radiation Units & Measurements, Bethesda, MD; 1993. 10.1118/1.597396
5. Podgorsak, E.B. (2005) Radiation Oncology Physics: A Handbook for Teachers and Students. IAEA, Vienna.
6. Joiner MC, Bentzen SM. Time-dose relationships: the linear-quadratic approach. In: Steel GG, editor. *Basic clinical radiobiology*. 3rd ed. London: Oxford University Press; 2002. pp. 120–133.
7. U. International Commission on Radiation, Measurements, Prescribing, recording, and reporting brachytherapy for cancer of the cervix (ICRU Report 89). Bethesda, Place Published; 2013.

8. Swamidas J., Kirisits C., De Brabandere M., Hellebust T.P., Siebert F.A., Tanderup K. Image registration, contour propagation and dose accumulation of external beam and brachytherapy in gynecological radiotherapy. Radiother Oncol. 2020;143:1–11. doi: 10.1016/j.radonc.2019.08.023. - DOI - PubMed
9. Oh S, Kim S. Deformable image registration in radiation therapy. Radiat Oncol J. 2017 Jun;35(2):101-111. doi: 10.3857/roj.2017.00325. Epub 2017 Jun 30. PMID: 28712282; PMCID: PMC5518453.
10. Brock KK, Mutic S, McNutt TR, Li H, Kessler ML (2017) Use of image registration and fusion algorithms and techniques in radiotherapy: report of the AAPM Radiation Therapy Committee Task Group No. 132. Med Phys 44:e43–e76. https://doi.org/10.1002/mp.12256 - DOI - PubMed
11. Tim Fox, George Andl, Soham Bose (2018) Velocity and Deformable image registration.
12. Rueckert D, Sonoda LI, Hayes C, Hill DL, Leach MO, Hawkes DJ. Nonrigid registration using free-form deformations: application to breast MR images. IEEE Trans Med Imaging. 1999 Aug;18(8):712-21. doi: 10.1109/42.796284. PMID: 10534053.
13. Nkiwane KS, Andersen E, Champoudry J, de Leeuw A, Swamidas J, Lindegaard J, et al. Total reference air kerma can accurately predict isodose surface volumes in cervix cancer brachytherapy. A multicenter study. Brachytherapy 2017;16:1184–91.
14. Serban M, Kirisits C, Pötter R, et al. Isodose surface volumes in cervix cancer brachytherapy: Change of practice from standard (Point A) to individualized image guided adaptive (EMBRACE I) brachytherapy Radiother Oncol 129:567–5742018 - PubMed
15. Andisco, D., Blanco, S., & Buzzi, A.E (2014). Dosimetry in Radiology. Revista Argentina de Radiologia (Online), 78(2), 114-117.

16. Jamema SV, Mahantshetty U, Andersen E, Noe KØ, Sørensen TS, Kallehauge JF, et al. Uncertainties of deformable image registration for dose accumulation of high-dose regions in bladder and rectum in locally advanced cervical cancer. Brachytherapy 2015;14:953–62.
17. van Heerden LE, Houweling AC, Koedooder K, et al. Structure-based deformable image registration: added value for dose accumulation of external beam radiotherapy and brachytherapy in cervical cancer. Radiother Oncol. 2017;123:319-324. - PubMed
18. Andersen ES, Noe KØ, Sørensen TS, et al. Simple DVH parameter addition as compared to deformable registration for bladder dose accumulation in cervix cancer brachytherapy. Radiother Oncol. 2013;107(1):52–57. doi: 10.1016/j.radonc.2013.01.013. - DOI - PubMed
19. Gerber R, Rink A, Croke J, Borg J, Beiki-Ardakani A, Fyles A, Milosevic M, Xie J, Keller H, Han K. Comparison of dosimetric parameters derived from whole organ and wall contours for bladder and rectum in cervical cancer patients treated with intracavitary and interstitial brachytherapy. Radiother Oncol. 2018 Jun;127(3):456-459. doi: 10.1016/j.radonc.2018.01.015. Epub 2018 Feb 6. PMID: 29426638.
20. Zakariaee R, Hamarneh G, Brown CJ, Spadinger I. Validation of non-rigid point-set registration methods using a porcine bladder pelvic phantom. Phys Med Biol. 2016 Jan 21;61(2):825-54. doi: 10.1088/0031-9155/61/2/825. Epub 2016 Jan 7. PMID: 26740511.
21. Abe, T., Tamaki, T., Makino, S. *et al.* Assessing cumulative dose distributions in combined radiotherapy for cervical cancer using deformable image registration with pre-imaging preparations. *Radiat Oncol* **9,** 293 (2014). https://doi.org/10.1186/s13014-014-0293-4
22. B.A. Esche, J.M. Crook, J.-C. Horiot, Dosimetric methods in the optimization of radiotherapy for carcinoma of the uterine cervix, International Journal of Radiation Oncology • Biology • Physics, 13 (1987) 1183-1192.
23. R. Pötter, T.H. Knocke, C. Fellner, M. Baldass, A. Reinthaller, H. Kucera, Definitive radiotherapy based on HDR brachytherapy with iridium 192 in uterine cervix carcinoma:

report on the Vienna University Hospital findings (1993–1997) compared to the preceding period in the context of ICRU 38 recommendations, Cancer/Radiothérapie, 4 (2000) 159-172.

24. J.M. Crook, B.A. Esche, G. Chaplain, J. Isturiz, I. Sentenac, J.C. Horiot, Dose-volume analysis and the prevention of radiation sequelae in cervical cancer, Radiotherapy and oncology : journal of the European Society for Therapeutic Radiology and Oncology, 8 (1987) 321-332.
25. I. Barillot, J.-C. Horiot, P. Maingon, G. Truc, G. Chaplain, J. Comte, J.-P. Brenier, Impact on treatment outcome and late effects of customized treatment planning in cervix carcinomas: baseline results to compare new strategies, International Journal of Radiation Oncology • Biology • Physics, 48 (2000) 189-200.
26. R. Hunter, J. Wilkinson, R. Swindell, Volume in intracavitary therapy; the first proof that it is clinically significant, Radiotherapy and Oncology, 64 (Suppl 1) (2002) S47-S48.
27. P.W. Grigsby, J.F. Williamson, K.S. Clifford Chao, C.A. Perez, Cervical tumor control evaluated with ICRU 38 reference volumes and integrated reference air kerma, Radiotherapy and Oncology, 58 (2000) 19-23.
28. R. Pötter, E. Van Limbergen, N. Gerstner, A. Wambersie, Survey of the use of the ICRU 38 in recording and reporting cervical cancer brachytherapy, Radiotherapy and Oncology, 58 (2001) 11-18.
29. K. Tanderup, S.K. Nielsen, G.B. Nyvang, E.M. Pedersen, L. Røhl, T. Aagaard, L. Fokdal, J.C. Lindegaard, From point A to the sculpted pear: MR image guidance significantly improves tumour dose and sparing of organs at risk in brachytherapy of cervical cancer, Radiotherapy and oncology : journal of the European Society for Therapeutic Radiology and Oncology, 94 (2010) 173-180.

30. R. Pötter, K. Tanderup, C. Kirisits, A. de Leeuw, K. Kirchheiner, R. Nout, L.T. Tan, C. Haie-Meder, U. Mahantshetty, B. Segedin, P. Hoskin, K. Bruheim, B. Rai, F. Huang, E. Van Limbergen, M. Schmid, N. Nesvacil, A. Sturdza, L. Fokdal, N.B.K. Jensen, D. Georg, M. Assenholt, Y. Seppenwoolde, C. Nomden, I. Fortin, S. Chopra, U. van der Heide, T. Rumpold, J.C. Lindegaard, I. Jürgenliemk-Schulz, The EMBRACE II study: The outcome and prospect of two decades of evolution within the GEC-ESTRO GYN working group and the EMBRACE studies, Clinical and Translational Radiation Oncology, 9 (2018) 48-60.
31. International Commission on Radiation Units and Measurements (ICRU) Report 38 (1985). Dose and volume specification for reporting intracavitary brachytherapy in gynecology